Master's thesis

NTNU
Norwegian University of Science and Technology
Faculty of Natural Sciences
Department of Physics

Alv Johan Skarpeid

Diffusive Curved Superconductor-Ferromagnet Proximity Systems in and out of Equilibrium

Master's thesis in Nanotechnology
Supervisor: Sol H. Jacobsen
Co-supervisor: Henning Goa Hugdal
July 2022

NTNU
Norwegian University of Science and Technology

Alv Johan Skarpeid

Diffusive Curved Superconductor-Ferromagnet Proximity Systems in and out of Equilibrium

Master's thesis in Nanotechnology
Supervisor: Sol H. Jacobsen
Co-supervisor: Henning Goa Hugdal
July 2022

Norwegian University of Science and Technology
Faculty of Natural Sciences
Department of Physics

NTNU
Norwegian University of
Science and Technology

ABSTRACT

In junctions between superconductors and ferromagnets, superconducting correlations may penetrate a short distance into the ferromagnet; this is the superconducting proximity effect. Heterostructures exhibiting the superconducting proximity effect may under the right conditions generate spin-polarized superconducting correlations that penetrate far into the ferromagnet; these are the long range triplet correlations. Supercurrents carried by long range triplets carry net spin, and may allow us to manipulate the magnetic structure of materials without the heat-loss of conventional electronics.

Introducing curvature to these heterostructures is a candidate for the generation of long range triplet correlations, and comes with the advantages that it is in principle dynamically tuneable and not directly dependent on intrinsic properties of the material.

In this thesis, we investigate the properties of curved superconductor-ferromagnet heterostructures in the diffusive regime. We reformulate the Usadel equation with a non-zero spin orbit field for 1D planar curves, as well as the quantum kinetic equations for investigating the non-equilibrium properties of the system. Furthermore, we introduce an arc length parametrization for a class of curves of non-uniform curvature to investigate the effects of non-uniform curvature on the system.

Analysis of the equilibrium supercurrent predict a curvature-induced amplification of the total charge current, that depending on the symmetry of the curved region the addition of curvature could induce a $0-\pi$ transition. The $0-\pi$ transition is also indicated to appear at different amplitudes of curvature depending on the symmetry of the curved region. A curvature induced $0-\pi$ transition is in principle dynamically tuneable, and thus promising for spintronic applications.

Analysis of the spin accumulation of a curved wire revealed curvature dependent spin accumulation profiles that could be further manipulated by an applied voltage bias; this may open new degrees of freedom in manipulating spintronic devices. The framework may also facilitate further investigation into non-equilibrium effects in superconductor heterostructures.

SAMMENDRAG

I strukturer med superledere og ferromagneter kan superledende korrelasjoner lekke et lite stykke inn i ferromagneten; dette er den superledende proksimitetseffekten. Hybridsystemer hvor denne effekten er signifikant kan ved de rette omstendighetene gi opphav til spinn-polariserte superledende korrelasjoner som penetrerer et langt stykke inn i ferromagneten. Dette er lik-spinn triplett korrelasjoner. Superstrømmer av disse lik-spinn triplettene har netto spinn, slik at de kan la oss manipulere den magnetiske strukturen til materialer uten varmetapet fra konvensjonell elektronikk.

Å krumme disse hybridstrukturene kan være en måte å generere lik-spinn triplett korrelasjoner. Krumning har fordelen at den i prinsippet er dynamisk justerbar, og ikke avhengig av iboende egenskaper i materalet.

I denne avhandlingen undersøkes egenskapene til krummede superleder-ferromgnet hybridstrukturer i regimet med diffusiv transport. Vi reformulerer Usadel-likningen med et endelig spin-bane juster-felt for endimensjonale kurver i planet, i tillegg til kvante-kinetiske likninger for å undersøke ikke-likevektsegenskapene til systemet. Videre introduserer vi en buelengde parametrisering av en klasse kurver, slik av vi kan studere effekten av ikke-uniform krumning.

Analyse av likevekt-superstrømmene viser en forsterkning av den totale ladningsstrømmen dersom systemet krummes. Avhengig av den geometriske symmetrien på systemet kan overgangen gjennomgå en $0-\pi$ overgang. Denne $0-\pi$ overgangen skjer ved forskjellige krumningsamplituder avhengig av symmetrien på den krummede regionen. En krumningsindusert $0-\pi$ overgang er i prinsippet dynamisk justerbar, og dermed lovende for anvendelser i spintronikk .

Analyse av spinn-akkumulering i en krummet ledning indikerer krummingsavhengige spinn-akkumuleringsprofiler, disse kan videre manipuleres ved å sette en spenning på systemet. Dette kan gi flere frihetsgrader for å manipulere kretselementer i spintronikk-systemer. Rammeverket kan også fasilitere videre undersøkelser av ikke-likevektseffekter i hybridstrukturer med superledere.

PREFACE

This thesis concludes the five-year programme in Nanotechnology with a specialization in Nanoelectronics at the Norwegian University of Science and Technology — and amounts to 30 ECTS-credits, and was carried out in the final semestre. The thesis is a continuation of a specialization project of 15 ECTS-credits carried out the previous semestre, both supervised by Dr. Sol Jacobsen and Dr. Henning Hugdal.

To ensure that all concepts novel to someone completing their degree in physics are introduced, parts of the specialization project thesis has been adpted to form parts of this thesis – these parts have been marked, and some relegated to appendices.

The scripts for solving the Usadel equation are available upon request, while a script for solving the Frenet-Serret equations is attached.

Typesetting was done in LaTeX, using my own modified version of the *arsclassica*-package. Most figures were made using Adobe Illustrator. Most of the numerical work is done in MATLAB, using the *bvp6c* package. This is a 6th order extention of the *bvp4c* package, implementing a 6th order collocation formula.

There are several people who have contributed to this thesis. First and foremost, I should be thanking my supervisors Henning and Sol for guidance and motivation. I would also like to thank Tancredi Salamone and Dr. Morten Amundsen, for our weekly meetings on curved systems. I am naturally grateful for the input to my own project, but also for letting me into their own work and introduction to less-talked-about-concepts like responding to peer review.

Finally, I should thank my classmates for our lunch breaks, communal coffee and course spesific inside jokes.

ALV JOHAN SKARPEID
TRONDHEIM, JULY 2022

NOTATION AND UNITS

Largely, this thesis will adhere to the conventions in physics — and most mathematical quantities are introduced when they appear in the text.

Scalar quantities are written using a different typeface than the body copy, as such $a, b, c, \alpha, \beta, \gamma$. Vector quantities are usaually written with a bold font in the same typeface $\mathbf{a}, \mathbf{b}, \mathbf{c}, \boldsymbol{\alpha}, \boldsymbol{\beta}, \boldsymbol{\gamma}$. The exception is the quantities in spin-, Nambu $\otimes$ spin- and Keldysh-space, which are written with $\underline{\cdot}$, $\hat{\cdot}$ and $\check{\cdot}$ respectively. At times, quantities of incompatible spaces are added, subtracted of multiplied, in which case the quantity of the lowest dimension should be raised to the right dimension by means of the Kronecker product with the relevant identity matrix.

There are some quantities and operations that appear throughout the text. The Pauli matrices are given as

$$\sigma_0 = \begin{pmatrix} 1 & 0 \\ 0 & 1 \end{pmatrix}, \quad \sigma_1 = \begin{pmatrix} 0 & 1 \\ 1 & 0 \end{pmatrix},$$
$$\sigma_2 = \begin{pmatrix} 0 & -i \\ i & 0 \end{pmatrix}, \quad \sigma_3 = \begin{pmatrix} 1 & 0 \\ 0 & -1 \end{pmatrix},$$

with $\tau_{1,2,3}$ being the corresponding matrices for Nambu space. Furthermore, we will mark quantities in spin- , Nambu$\otimes$spin and Keldysh space with $\underline{\cdot}$, $\hat{\cdot}$, $\check{\cdot}$ respectively. At times, we will simplify some of this notation as to not clutter the equations – this will be made clear in the context.

As is convention, we will be using natural units with

$$c = \epsilon_0 = \mu_0 = \hbar = k_B = 1.$$

Here, c is the speed of light, ϵ_0 is the vacuum permittivity, μ_0 is the vacuum permeability, $\hbar$ the reduced Planck constant and k_B Boltzmann's constant.

CONTENTS

1 INTRODUCTION

At its discovery in the early twentieth century, superconductivity was a phenomenon right at the fringes of the applied natural sciences; the temperatures required for the phenomenon to manifest were impractial and the phenomenon largely not understood for decades. Today however, superconductors have found applications as electromagnets[1], integral parts of precise measurement devices [2] and as a candidate materials in unconventional computing systems.

Spesifically, we are concerned with *superconducting spintronics* [3, 4]. Spintronics, in its most general form, considers manipulating the degrees of freedom of a system related to spin. For a more concrete picture, one might picture spin currents replacing charge currents in logical circuits.

The effects present in a spintronic system can be enhanced by introducing superconductivity, e. g. it is possible to spin polarize a supercurrent. These have the potential to carry net spin — crucially without the heat loss of a conventional (spin polarized) current. Spesifically, we are in this thesis concerned with the generation of such spin polarized supercurrent in *curved superconductor-ferromagnet heterostructures*.

Taking a step back, superconductivity and magnetism are in some sense antagonistic phenomena. Superconductors expel weak magnetic fields, and strong magnetic fields makes materials transition away from the superconducting state. However, on the *mesoscopic* scale, the phenomena may coexist.

In junctions between superconductors and ferromagnets, electron pairs from the superconductor of zero spin may be able to penetrate far into the ferromagnet if the electron pair is converted to the state where both electron spins align with the field — we refer to the former configuration as the *spin singlet* state, and the latter as the *equal spin triplet* or *long range triplet* state. The equal spin triplets come with a hope of dissipationless net-spin currents; in turn this may allow us to manipulate the magnetic structure of materials without the heat-loss of conventional electronics.

There are several conceptual ways of generating the long-range triplets. Ideally, such a method should be easy to implement experimentally and allow for precice control of the long range triplet current. Curved structures, which is the subject of this thesis, may be a candidate to fill some of the gaps of these other concepts.

1.1 Fundamental concepts

SUPERCONDUCTIVITY In 1911, while measuring the temperature dependence of resistivity in mercury, H. Kamerlingh-Onnes found the sample resistance to disappear below ~4 K; this phenomenon is called superconductivity [5]. More precicely, superconducting materials exhibit no electric resistivity and expel magnetic flux below a critical temperature, T_c – this is the *Meissner effect*.

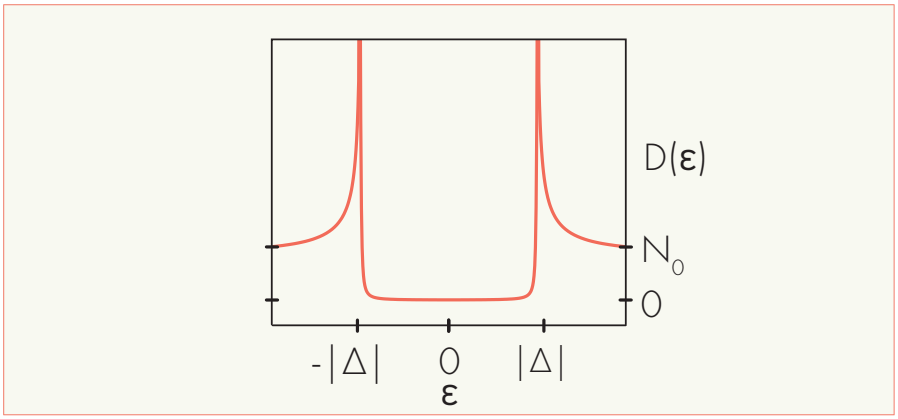

Figure 1.1: Density of states in a bulk BCS superconductor. The horisontal axis gives the energy level, ε, with $\varepsilon = 0$ being the Fermi level. The vertical axis gives the density of states with N_0 being density of states in a normal metal at the Fermi level, N_0. In a bulk superconductor, a gap of size $2|\Delta|$ appears around the Fermi level.

We are concerned with conventional BCS superconductors [6]. Here, an attractive potential between two electrons creates bound electron pairs called *Cooper pairs*; these in turn form a condensate. BSC superconductors exhibit *s-wave* symmetry, meaning the order parameter is spherically symmetric in momentum space. Also, the electrons forming a Cooper pair are of opposite momenta and spin.

Given a condensate of Cooper pairs, we may perform a mean-field approximation, allowing us to characterize it using a complex order-parameter, $\Delta = |\Delta| \cdot e^{i\phi}$. We sometimes refer to $|\Delta|$ as the *superconducting gap*[1] - as a gap of magnitude $|\Delta|$ opens at each side of the Fermi level in a bulk superconductor. We refer to ϕ as the *superconducting phase*. For a single superconductor, the phase may be removed from the Hamiltonian of the system by means of a $U(1)$ gauge transformation, but a phase difference can give rise to a *supercurrent* in a junction [7].

For a more thorough introduction to superconductivity, a textbook like ref. [7] may be a good place to start.

FERROMAGNETISM In a *ferromagnetic* material, the magnetic moments of the materials tend to align; spesifically, the *exchange interaction* favors the alignment of the electron spins [8]. Analogous to the superconductor, the ferromagnetic state can be characterized by an order parameter, $\mathbf{h}$, which we refer to as the exchange field. As the material is heated to the *Curie-Weiss* temperature, ferromagnetic order vanishes and the exchange field becomes zero [9]. In a mean-field approximation the exchange field couples to the electron spin, creating spin-dependent energy levels. We refer to this as the *spin-splitting* of the (electron) energy levels [8, 10].

PROXIMITY EFFECT When a superconductor is placed in proximity to a (ferromagnetic) metal, the Cooper pairs of the superconductor may in some

1 The term superconducting gap is sometimes used to denote Δ. For clarity, the absolute magnitude of the gap is 2Δ.

sense leak into the metal. This induces superconducting-like behaviour in the metal, and is ultimately the main focus of this thesis.

Spesifically, we can understand the effect in terms of *Andreev reflection* [11, 12]. Here, on the metal side of the interface, an electron hits the interface and a hole is *retroreflected* and a Cooper pair is formed inside the superconductor. The process is reversible, in the sense that we may consider a Cooper pair meeting a hole at the interface. The Cooper pair and hole are annihilated, and the hole retroreflects an electron.

The Andreev reflection induces superconducting like behaviour in the magnetic region. This is manifested in, e. g., that a small gap opens up in the density of states – resembling that of a superconductor. Furthermore, the states induced in the metal by the superconductor, the *Andreev states*, may carry e. g. supercurrents. However, over longer distances, these states decohere and the effects of the superconductor disappears. In the absence of a spin splitting field, the superconducting correlations decay over a distance called the *(superconducting) coherence length*, ξ, which is typically on the order of $\sim 10 - 1000$ nm, depending on the material, e. g., the temperature. [8]. With magnetic order present the spin structure of the superconducting correlations determine the rate of the decay, and hence the coherence length.

In a conventional BCS superconductor, the induced state is of the *spin-singlet* type, given as $|\uparrow\downarrow\rangle - |\downarrow\uparrow\rangle$[2]; these carry no spin and decohere rapidly in the presence of an exchange field, $\mathbf{h}$. A simple picture is, as written in the introduction, that an exchange field tends to align spins – which is ultimately incompatible with the singlet state. For a more detailed picture, the exchange field splits the energy levels of the electrons forming the Cooper pair. This in turn gives the Cooper pair a finite, i. e. non-zero, *center of mass momentum*, which is moulated, i. e. it decays, in real space. [13]

Explicitly, the splitting of the energy levels induces an FFLO[3]-like state, where each of the terms pick up the opposite phase factor as it penetrates into the ferromagnet [13]. This generates a superconducting correlation of the *opposite spin* or *short range triplet*, $|\uparrow\downarrow\rangle + |\downarrow\uparrow\rangle$, state – and converts said state back to the singlet state oscillatory. We refer to this process as *spin mixing*.

While the projection of the opposite spin triplet onto the spin quantization axis is zero, it does have a net spin if projected onto some non-colinear spin quantization axis. Explicitly, the state $|\uparrow\downarrow\rangle + |\downarrow\uparrow\rangle$ becomes some linear combination of $|\uparrow\uparrow\rangle$ and $|\downarrow\downarrow\rangle$ states along some non-colinear spin quantization axis. We refer to these states as *equal spin triplets* or *long range triplets*. If, e. g., the $|\uparrow\uparrow\rangle$ state aligns with the exchange field, the energy levels of the electrons are not split by the exchange field – meaning they are able to penetrate far into the ferromagnetic regions.

A conceptually simple way to change the spin quantization axis would be a multilayered structure, with non-colinear magnetization of the ferromagnetic layers [16, 17]. Another approach is that of refs. [18, 19], utilizing a helical magnetization of the magnetized region. For a qualitative discussion of the generation of spin polarized supercurrents from superconductor-ferromagnet structures, see e. g. ref. [20].

2 These states are to have a normalization factor of $1/\sqrt{2}$ This is a qualitative discussion, so we ignore these factors.

3 FFLO is an acromym for Fulde, Ferrell, Larkin, Ovchinnikov, who theorised the state [14, 15].

As a final note, the proximity effect is reciprocal; the superconductor is depleted of Cooper-pairs when placed in contact with, e. g., a metal. We will not consider this reverse effect, which is negligible for interfaces with low transparency.

SPIN ORBIT COUPLING In superconductor-ferromagnet sturctures, spin orbit coupling may also be a candidate for the generation of long range triplets [21, 22].[4]

Spin orbit coupling refers to the coupling of the quasiparticle momentum, $\mathbf{p}$, to its spin $\underline{\boldsymbol{\sigma}}$. A simple picture comes from considering an electron moving in an inhomogeneous potential. Performing a Lorentz transformation to the rest frame of the electron creates a term in the electron Hamiltonian that is linear in both spin and momentum.

There are different mechanisms for having spin orbit interactions. The examples typically presented in this context are those of Rashba and Dresselhaus spin orbit coupling. *Rashba* spin orbit coupling stems from some broken symmetry along one axis – typically near an interface in a thin structure [24]. *Dresselhaus* spin orbit coupling appears in materials where the crystal structure lacks inversion symmetry, with Dresselhaus' spesific example being the zinc blende structure [25].

1.2 Structure and scope

In this thesis, we are considering diffusive superconductor–ferromagnet with in-plane curvature. More spesifically, we are investigating how curvature effects density of states, equilibrium and non-equilibrium spin accumulation and current.

In the second chapter, we are recapitulating quasiclassical theory for superconductor–ferromagnet systems, arriving at the *Usadel equation*. The third chapter introduces curved systems and the necessary notation for desicribing them, while fourth chapter adapts the Usadel equation to these systems both in and out of equilibrium. In the fith chapter, we are introducing the classes of curves we are to study as well as the physical observables which we are to study. These geometries are, in addition to the straight default case, a circular arc and some with curvature functions given by linear combinations of logistic functions, while the physical observables are the equilibrium current and magnetization in and out of equilibrium. We show our findings in chapter 6, and summarise in chapter 7.

4 While we will be considering only diffusive structures, this also holds in the ballistic regime [23].

2 QUASICLASSICAL THEORY FOR SUPERCONDUCTING PROXIMITY SYSTEMS

This chapter introduces the notation and main assumptions of quasiclassical theory for superconducting proximity systems.

The motivation is that most observables can be calculated from the *Green's function* of the system – meaning we should be able to estimate observables by solving the equation of motion for the Green's function.

Deriving such an equation, and writing it in a tractable form, is ultimately out of the scope of this thesis. For the brief version, we start with free electrons, where finding the exact Green's function is not very difficult. We may write an equation for first order correction to the Green's function of the free electrons, this will be *Gor'kov's equation* [26]. However, solving Gor'kov's equation is impractical for most systems. The two key assumptions to arrive at some tractable form of an equation of motion will be the *quasiclassical approximation*[27, 28] — where we confine the problem to be close to the Fermi surface and integrate over the most rapid (spatial) oscillations of the (exact) Green's function — and that of *diffusive transport*. Applying the quasiclassical approximation gives the *Eilenberger equation* [29], while the additional assumption of diffusive transport gives the *Usadel equation* [30].

2.1 Green's Functions

For very simple systems, it may be helpful to look at the Green's function as the inverse (operator) of the differentiation operator. This picture ceases to be helpful for more complicated systems. Another, more generally applicable picture, is to define the Green's function as the expectation value of a product of field operatores

$$G_{\sigma_1\sigma_2}(\mathbf{x}_1, \mathbf{x}_2) = -i\langle n|\hat{\psi}_{\sigma_1}(\mathbf{x}_1)\hat{\psi}^\dagger_{\sigma_2}(\mathbf{x}_2)|n\rangle. \tag{2.1}$$

Here, $\mathbf{x}_j$ is the spatial and temporal coordinates, $\hat{\psi}$ the field operator, σ_j a spin-index and $|n\rangle$ some quantum state. The typical way to think about these is that we inject some particle at $\mathbf{x}_2$, have the system propagate in time, and attempt to remove the particle at $\mathbf{x}_1$. This comes with the caveat that particles are interchangable; we have no guarantee that we are attempting to measure the same particle. A more accurate picture may be that the Green's function, G, is a measure associated with probability of a particle propagating from $\mathbf{x}_2$ to $\mathbf{x}_1$.

For superconductor-ferromagnet systems, we chose, analogous to ref. [31], field operators of the form

$$\hat{\Psi}_j = \begin{pmatrix} \hat{\psi}_{j\uparrow} \\ \hat{\psi}_{j\downarrow} \\ \hat{\psi}^\dagger_{j\uparrow} \\ \hat{\psi}^\dagger_{j\downarrow} \end{pmatrix}, \quad \hat{\Psi}^\dagger_j = \begin{pmatrix} \hat{\psi}^\dagger_{j\uparrow} & \hat{\psi}^\dagger_{j\downarrow} & \hat{\psi}_{j\uparrow} & \hat{\psi}_{j\downarrow} \end{pmatrix}, \tag{2.2}$$

where j is a coordinate index, i. e. $\hat{\psi}_{j\sigma} = \psi_\sigma(x_j)$. These act on Nambu$\otimes$ spin space[1], meaning $\hat{\psi}^\dagger_{j\sigma}$ is the creation operator for an electron with spin σ. Note that this is different from e. g. refs. [27, 31], which do not concern themselves with the spin stucture — meaning the field operators act only on particle-hole space.

We will not be writing Gor'kov's equation in terms of eq. (2.1), but rather in terms of the *retarded, advanced* and *Keldysh* Green's functions, $\hat{G}^R, \hat{G}^A, \hat{G}^K$ [31–33]. We define them as

$$\hat{G}^R = -i\hat{\tau}_3 \left\langle \hat{\Psi}_1 \hat{\Psi}_2^\dagger + \left(\hat{\Psi}_2^{\dagger T} \hat{\Psi}_1^T\right)^T \right\rangle \theta(t_1 - t_2), \tag{2.3a}$$

$$\hat{G}^A = +i\hat{\tau}_3 \left\langle \hat{\Psi}_1 \hat{\Psi}_2^\dagger + \left(\hat{\Psi}_2^{\dagger T} \hat{\Psi}_1^T\right)^T \right\rangle \theta(t_2 - t_1), \tag{2.3b}$$

$$\hat{G}^K = -i \left\langle \hat{\Psi}_1 \hat{\Psi}_2^\dagger - \left(\hat{\Psi}_2^{\dagger T} \hat{\Psi}_1^T\right)^T \right\rangle, \tag{2.3c}$$

where $\theta(t)$ is the Heaviside step function, and t_i the temporal coordinate. The retarded and advanced Green's functions are causal and anti-causal respectively, i. e. for the advanced Green's function we attempt to remove the particle at a later time than we earlier it, having it propagating backwards in time. The Keldysh component gives information on the occupancy of the states, although in a convoluted way. This can be realized from the fact that each of the terms in eq. (2.3c) look similar to a single particle density operator if the field operators act at the same time and position.

There is some redundancy in the definition of the Green's functions, which relates to the physical interpretation of the components of the Green's function. We start by considering eq. (2.2) and the matrix product

$$\hat{\Psi}_1 \hat{\Psi}_2^\dagger = \begin{pmatrix} \hat{\psi}_{1\uparrow}\hat{\psi}^\dagger_{2\uparrow} & \hat{\psi}_{1\uparrow}\hat{\psi}^\dagger_{2\downarrow} & \hat{\psi}_{1\uparrow}\hat{\psi}_{2\uparrow} & \hat{\psi}_{1\uparrow}\hat{\psi}_{2\downarrow} \\ \hat{\psi}_{1\downarrow}\hat{\psi}^\dagger_{2\uparrow} & \hat{\psi}_{1\downarrow}\hat{\psi}^\dagger_{2\downarrow} & \hat{\psi}_{1\downarrow}\hat{\psi}_{2\uparrow} & \hat{\psi}_{1\downarrow}\hat{\psi}_{2\downarrow} \\ \hat{\psi}^\dagger_{1\uparrow}\hat{\psi}^\dagger_{2\uparrow} & \hat{\psi}^\dagger_{1\uparrow}\hat{\psi}^\dagger_{2\downarrow} & \hat{\psi}^\dagger_{1\uparrow}\hat{\psi}_{2\uparrow} & \hat{\psi}^\dagger_{1\uparrow}\hat{\psi}_{2\downarrow} \\ \hat{\psi}^\dagger_{1\downarrow}\hat{\psi}^\dagger_{2\uparrow} & \hat{\psi}^\dagger_{1\downarrow}\hat{\psi}^\dagger_{2\downarrow} & \hat{\psi}^\dagger_{1\downarrow}\hat{\psi}_{2\uparrow} & \hat{\psi}^\dagger_{1\downarrow}\hat{\psi}_{2\downarrow} \end{pmatrix}. \tag{2.4}$$

Here, the lower half is essentially the conjugate of the top half. This redundancy carries over to eq. (2.3), and we rewrite the Green's functions, $\hat{G}^A, \hat{G}^R, \hat{G}^K$ as

$$\hat{G}^R = \begin{pmatrix} \underline{G}^R & \underline{F}^R \\ (\underline{F}^R)^* & (\underline{G}^R)^* \end{pmatrix}, \tag{2.5a}$$

$$\hat{G}^A = \begin{pmatrix} \underline{G}^A & \underline{F}^A \\ (\underline{F}^A)^* & (\underline{G}^A)^* \end{pmatrix}, \tag{2.5b}$$

$$\hat{G}^K = \begin{pmatrix} \underline{G}^K & \underline{F}^K \\ -(\underline{F}^K)^* & -(\underline{G}^K)^* \end{pmatrix}. \tag{2.5c}$$

1 Nambu space is used interchangably with *particle-hole space.*

Here $\cdot^*$ means elementwise conjugation. The entries are essentially just encoding the spin-structure with

$$\underline{G}^{A,R,K} = \begin{pmatrix} G^{A,R,K}_{\uparrow\uparrow} & G^{A,R,K}_{\uparrow\downarrow} \\ G^{A,R,K}_{\downarrow\uparrow} & G^{A,R,K}_{\downarrow\downarrow} \end{pmatrix}, \tag{2.6a}$$

$$\underline{F}^{A,R,K} = \begin{pmatrix} F^{A,R,K}_{\uparrow\uparrow} & F^{A,R,K}_{\uparrow\downarrow} \\ F^{A,R,K}_{\downarrow\uparrow} & F^{A,R,K}_{\downarrow\downarrow}. \end{pmatrix} \tag{2.6b}$$

The entries of these matrices can be understood in terms of the "simple" picture for the Green's functions presented at the the beginning of the section. Note that for the F-components, i. e. the off-diagonal block of eq. (2.4), two creation or destruction operators are paired. We refer to the F-components as *anomalous Green's functions* — this is the part of the Green's function that describes the dynamics of the Cooper pairs, i. e. we expect them to be zero without the presence of superconducting correlations. For a more thorough derivation of the fundamentals, see refs. [27, 31]. For less detail oriented explanation of the fundamentals, see refs. [10, 34].

2.2 Quasiclassical Green's functions

The main approximation to arrive at a tractable form of the equation of motion for the Green's function is that of the *quasiclassical approximation*. For using the approximation, we make two key assumptions. The first is that the main contribution to the Green's function is due to quasiparticles near the Fermi surface, and the second that the spatial variations of our perturbations, e. g. scattering potentials, exchange fields or superconducting order, are slow compared to the Fermi wavelength, $\lambda_F = 2\pi/p_F$ – the Fermi momentum is p_F. In this section, we restate these assumptions with more rigour and sketch the transformation from exact Green's function, $\check{G}$, to quasiclassical Green's function, $\check{g}$. The section is loosely based on refs. [10, 27, 31, 34].

For a slightly more concrete picture, we want to move from $\check{G}(\mathbf{r}_1, t_1, \mathbf{r}_2, t_2)$ to $\check{g}(\mathbf{R}, \hat{\mathbf{p}}_F, \epsilon, t)$. Here $\mathbf{R}$ is the center-of-mass spatial coordinate, $\hat{\mathbf{p}}_F$ a unit vector on the Fermi surface, ϵ the quasiparticle energy and t the center-of-mass time coordinate.

We start by rewriting the Green's function in terms of the *mixed representation*[2] meaning $\check{G}(\mathbf{r}_1, t_1, \mathbf{r}_2, t_2) \to \check{G}(\mathbf{R}, t, \mathbf{s}, u)$, with

$$\mathbf{R} = \frac{\mathbf{r}_1 + \mathbf{r}_2}{2,} \tag{2.7a}$$

$$t = \frac{t_1 + t_2}{2}, \tag{2.7b}$$

$$\mathbf{s} = \mathbf{r}_1 - \mathbf{r}_2, \tag{2.7c}$$

$$u = t_1 - t_2. \tag{2.7d}$$

The physical interpretation of the relative variables, $\mathbf{s}, u$, is simpler if we perform a Fourier transform. For the Green's function, we have

$$\check{G}(\mathbf{R}, \mathbf{p}, \epsilon, t) = \int du\, e^{i\epsilon u} \int d\mathbf{s}\, e^{-i\mathbf{p}\cdot\mathbf{s}} \check{G}(\mathbf{R}, \mathbf{s}; t, u), \tag{2.8}$$

2 Sometimes refered to as the *Wigner representation* in the literature

with the sign-convention inherited from ref. [27].

This transformation is exact, and we may introduce the approximation, first assuming the main contribution to the Green's function is close to the Fermi surface. Spesifically, introduce

$$\check{G} = \check{G}_{\text{low}} + \check{G}_{\text{high}}, \tag{2.9}$$

where the subscripts refer to a low and high energy part of the Green's function. The assumption becomes that $\check{G}_{\text{low}} \gg \check{G}_{\text{high}}$ and

$$\check{G}_{\text{low}} = \begin{cases} \check{G} & \text{if } |\xi_{\mathbf{p}}| < \delta\epsilon \\ 0 & \text{otherwise} \end{cases}. \tag{2.10}$$

Here, $\delta\epsilon$ is some small cut-off energy and $\xi_{\mathbf{p}} = \mathbf{p}^2/2m - \mu$ is the kinetic energy relative to the Fermi level. Here, m is the electron mass and μ the chemical potential. The assumption is a little more subtle, and treated more rigorously in ref [35]. We have to keep in mind that we are to not only transforming the Green's function, but also Gor'kov's equation. This definition, with $\delta\epsilon$ of eq. (2.10) as just a book-keeping device essentially allows us to retrace the steps required for deriving Gor'kov's equation in the quasiclassical regime.

We may now define the quasiclassical Green's function as

$$\check{g}(\mathbf{R}, \hat{\mathbf{p}}_F, \epsilon, t) = \frac{i}{\pi} \int_{-\delta\epsilon}^{\delta\epsilon} d\xi_p \, \check{G}(\mathbf{R}, \mathbf{p}, \epsilon, t). \tag{2.11}$$

The prefactor, i/π, is to ensure that the quasiclassical Green's function is normalized, with $\check{g} \cdot \check{g} = 1$. The conventions vary here, and we have inherited this one from ref [27]. Common for all choices of transformation is the introduction of an imaginary prefactor; hence the matrix elements will change sign under complex conjugation.

The quasiclassical counterpart to eq. (2.5) then becomes

$$\check{g} = \begin{pmatrix} \hat{g}^R & \hat{g}^K \\ 0 & \hat{g}^A \end{pmatrix}, \tag{2.12a}$$

$$\hat{g}^R = \begin{pmatrix} \underline{g}^R & \underline{f}^R \\ -\underline{\tilde{f}}^R & -\underline{\tilde{g}}^R \end{pmatrix}, \tag{2.12b}$$

$$\hat{g}^A = \begin{pmatrix} \underline{g}^A & \underline{f}^A \\ -\underline{\tilde{f}}^A & -\underline{\tilde{g}}^A \end{pmatrix}, \tag{2.12c}$$

$$\hat{g}^K = \begin{pmatrix} \underline{g}^K & \underline{f}^K \\ \underline{\tilde{f}}^K & \underline{\tilde{g}}^K \end{pmatrix}. \tag{2.12d}$$

The $\tilde{\cdot}$ operator encodes elementwise complex conjugation, $i \to -i$ and energy $\epsilon \to -\epsilon$. The sign change of the energy can be understood from performing the Fourier transformation to energy/momentum coordinates on each element of, e. g. $\hat{G}^R$.

2.3 Quasiclassical equations of motion

With a quasiclassical Green's function, we also need a quasiclassical analogue of the Gor'kov equation [26]; this will be the *Eilenberger equation* [29]. Rigorously deriving the Eilenberger is involved, so we will state Gor'kov's equation and point out the approximations.

The Gor'kov equation is given as

$$\left[G_{(0)}^{-1}, \check{G}\right]^{\bullet} = \left[\check{\Sigma}, \check{G}\right]^{\bullet}, \tag{2.13}$$

with

$$\check{G} = \begin{pmatrix} \check{G}^{R} & \check{G}^{K} \\ 0 & \check{G}^{A} \end{pmatrix}, \tag{2.14}$$

where $\bullet$ is an associative binary operator encoding the integral over spatial and temporal coordinates of the matrix product of the operands and $G_{(0)}^{-1}$ is the differential operator of the unperturbed system, i. e. that of a free quasiparticle. Specifically, we have

$$G_{(0)}^{-1} = +i\hat{\tau}_3 \frac{\partial}{\partial t} + \frac{\nabla^2}{2m} + \mu \tag{2.15}$$

where j is the coordinate index, meaning $G_{(0)j}^{-1}$ acts on field operator j, μ and ∇ acting only on the spatial coordinates.[3] The factor $\hat{\tau}_3 = \mathrm{diag}(1, 1, -1, -1)$ appears because the top (left) block in Nambu $\otimes$spin-space corresponds to electrons, while the bottom (right) corresponds to holes.

The brief idea is that the transformations of the quasiclassical approximation will allow us to rewrite $G_{(0)}^{-1}$ into a tractable form, which along with the gradient approximation [27, 35], essentially just the first Taylor-expansion, and the spatial integrals of the Forier transformation will allow us to simplify the bullet product, $\bullet$.

More spesifically, the differential operator written out in terms of the mixed representation becomes

$$G_{(0)j}^{-1} = +i\hat{\tau}_3\left(\frac{1}{2}\partial_t \pm \partial_u\right) + \frac{1}{2m}\left(\frac{1}{4}\nabla_R^2 \pm \nabla_R \cdot \nabla_s + \nabla_r^2\right) + \mu, \tag{2.16}$$

with the $\pm$ signs corresponds to which coordinate indices we are acting on, i. e. which set of field operators. With the Fourier transformation of the relative coordinates, the operators change with $\partial_u \to -i\epsilon, \nabla_s \to i\mathbf{p} = im\mathbf{p}$. Furthermore, we will be neglecting the second derivative with respect to the spatial center-of-mass coordinate, $\mathbf{R}$. If we also are to neglect the center-of-mass time derivative, the integration over temporal coordinates of the bullet-product, $\bullet$, becomes trivial, and we may simply neglect it. This corresponds to only considering steady state system. The end result is the *Eilenberger equation* [29], which we write as

$$\left[\check{\Sigma}, \check{g}\right] + iv_F\hat{\mathbf{p}}_F\nabla_{\mathbf{R}}\check{g} = 0, \tag{2.17}$$

where we have made the substitution $\mathbf{p} \to v_F\hat{\mathbf{p}}_F$, as the momentum is confined to the Fermi surface.

3 This glosses over some subtleties regarding which set of coordinates the inverse Green's function acts on. This is made clearer in ref. [31]

We will however be considering systems with diffusive quasiparticle transport. Physically, this corresponds to the effect of elastic scattering on impurities to be strong. A more precise description is that the mean free path of the quasiparticles is small compared to the other length scales, except the Fermi wavelength, λ_F, in the problem. In making the quasiclassical approximation, the Green's function is confined to the Fermi surface, such that $\check{g}$ is a function of $\hat{\mathbf{p}}_F$, and not $\mathbf{p}$ itself. If the transport is diffusive, this dependence will be averaged over the whole Fermi surface. From looking at the Eilenberger equation, eq. (2.17), we should be able to eliminate the two degrees of freedom associated with the direction of the momentum, $\hat{\mathbf{p}}_F$. We will however be incurring the "cost" of another gradient operator.

To avoid any confusion relating to the matrix forms, and which space the operators are acting on, we will be sketching the derivation only for $\hat{g}^R$, which we will write as $\hat{g}$ for brevity. The sketch of the derivation is based on ref. [31] and to a lesser degree ref. [27].

With the assumed short mean field path, we may expand the quasiclassical Green's function in momentum, which is essentially an expansion in spherical harmonics

$$\hat{g}(\mathbf{R}, \hat{\mathbf{p}}_F, \epsilon, t) = \hat{g}_s(\mathbf{R}, \epsilon, t) + \hat{\mathbf{p}}_F \cdot \hat{\mathbf{g}}_p(\mathbf{R}, \epsilon, t). \tag{2.18}$$

In this expansion, $\hat{g}_s$ is the isotropic part of the quasiclassical Green's function, $\hat{\mathbf{g}}_p$ is the anisotropic part[4], where the anisotropy is assumed linear in the direction of $\hat{\mathbf{p}}_F$, i. e. the direction of transport. The vector $\hat{\mathbf{p}}_F$ is still a unit vector at the Fermi surface pertaining to our quasiparticle. Implicitly, we are then assuming $\hat{\mathbf{g}}_p^2$ to be negligible due to the strong disorder.

It must be stressed that the argument is more nuanced than $\hat{g} \to \hat{g}_s$. It may be helpful to think about eq. (2.18) as transforming the Eilenberger equation, eq. (2.17), into two coupled equations for $\hat{g}_s$ and $\hat{\mathbf{g}}_p$. With some further assumptions, chiefly that isotropic elastic scattering dominates, we may write the non-isotropic part of the quasiclassical Green's function, $\hat{\mathbf{g}}_p$, in terms of the isotropic part, and insert this back into the Eilenberger equation. The result will be the Usadel equation [30], where only $\hat{g}_s$ enters explicitly.

The way the Usadel equation is derived in refs. [27, 31], the part of the self energy, $\hat{\Sigma}$, that depends on elastic scattering is expanded in spherical harmonics, analogous to eq. (2.18), with

$$\hat{\Sigma}_{\text{scattering}} = \hat{\Sigma}_s + \hat{\mathbf{p}}_F \cdot \hat{\mathbf{\Sigma}}_p, \tag{2.19}$$

where $\hat{\Sigma}_{s,p}$ are the isotropic and non-isotropic part of the (scattering) self energy function.

Specifically, we are assuming the elastic scattering to happen on a potential $U(\mathbf{p} - \mathbf{p}')$, where $\mathbf{p} = \hat{\mathbf{p}}_F$. Making the further assumption that the potential does not depend on the magnitude of the momentum, $\mathbf{p}$, we may write $U(\mathbf{p} \cdot \mathbf{p}')$. Then, the self energy function for elastic impurity scattering is given as [31]

$$\hat{\Sigma}_{\text{imp}}(\mathbf{p}) = n_i N_0 \int \frac{d\Omega_{p'}}{4\pi} |U(\mathbf{p} - \mathbf{p}')|^2 \hat{g}(\mathbf{p}'), \tag{2.20}$$

4 The subscripts s and p are used for historic reasons, and corresponds to s- and p- waves.

where $d\Omega_{p'}$ is the solid angle element. In the *Born approximation*, we may define the elastic scattering rate as

$$\frac{1}{\tau} = 2\pi n_i N_0 \int \frac{d\Omega_{p'}}{4\pi} |U(\mathbf{p}\cdot\mathbf{p}')|^2, \tag{2.21}$$

where n_i is the number of impurities per unit volume, and N_0 is the density of states (per spin) at the Fermi surface. This, along with the observation that

$$\hat{\mathbf{p}}_F \hat{\Sigma} = \hat{\mathbf{p}}_F \hat{\Sigma}_s + \hat{\mathbf{\Sigma}}_p, \tag{2.22}$$

allows us to separate the scalar quantities from the vector quantities such that we may find explicit expressions for $\hat{\Sigma}_s$ and $\hat{\mathbf{\Sigma}}_p$. The details of the calculation are given in refs. [27, 31], with the end results being

$$\hat{\Sigma}_s = -\frac{-i}{2\tau}\hat{g}_s, \tag{2.23a}$$

$$\hat{\mathbf{\Sigma}}_p = -\left[\frac{1}{\tau} - \frac{1}{\tau_{tr}}\right]\hat{\mathbf{g}}_p. \tag{2.23b}$$

where $1/\tau$ is the elastic scattering rate of eq. (2.21) and τ_{tr} is the *transport time*, defined by

$$\frac{1}{\tau_{tr}} = 2\pi n_i N_0 \int \frac{d\Omega_{p'}}{4\pi} |U(\mathbf{p}\cdot\mathbf{p}')|^2 (1 - \hat{\mathbf{p}}\cdot\hat{\mathbf{p}}'), \tag{2.24}$$

where n_i is the number of impurities per unit volume, an N_0 is the density of states at the Fermi surface. The introduction of τ_{tr} may seem unmotivated, but does appear in transport theory. For the introduction of the quantity in a different context, see e. g. the chapter on Fermi liquid theory of ref. [36].

We may now insert these expressions back into the Eilenberger equation, i. e. we combine eq. (2.17) with

$$\hat{\Sigma}_{total} = \hat{\Sigma} + \hat{\Sigma}_s + \hat{\mathbf{p}}_F \cdot \hat{\mathbf{\Sigma}}_p, \tag{2.25}$$

where $\hat{\Sigma}$ includes all other self energy terms, like that of superconducting order or an exchange field. This gives us an expression for the anisotropic part of the quasiclassical Green's function, $\hat{\mathbf{g}}_p$, in terms of the isotropic part, $\hat{g}_s$, with

$$\hat{\mathbf{g}}_p = -v_F \tau_{tr} \hat{g}_s \nabla_{\mathbf{R}} \hat{g}_s. \tag{2.26}$$

Explicitly, inserting eq. (2.25) into the Eilenberger equation gives

$$\left[\hat{\Sigma}, \hat{g}_s\right] - \frac{i v_F^2 \tau_{tr}}{3} \nabla_{\mathbf{R}} \cdot \left(\hat{g}_s \nabla \hat{g}_s\right). \tag{2.27}$$

We may write this more compactly by supressing the subscripts and introducing the *diffusion coefficient*[5]

$$D_F = \frac{1}{3} v_F^2 \tau_{tr}, \tag{2.28}$$

5 We spesifically assumed the mean free path to be small compared to the other length scales of the problem, the mean free path is $l = v_F \cdot \tau_{tr}$.

such that the equation of motion is given as

$$\left[\hat{\Sigma}, \hat{g}\right] = iD_F \nabla \cdot (\hat{g} \nabla \hat{g}) \,. \tag{2.29}$$

This is the *Usadel equation* [30]. Note that the self energy function, $\hat{\Sigma}$, has changed compared to eq. (2.17), as we have extracted the term related to elasic scattering. It is possible to carry out an analogous derivation with both elastic scattering and spin-flip scattering [27], but this is ultimately outside our scope. It should also be stressed that only the isotropic part of the Green's function enters explicitly into the equation, such that meaning the $\hat{g}$ of the Usadel and Eilenberger equation should not be conflated. The term $(\hat{g}\nabla\hat{g})$ is called the *matrix current*, with different conventions on sign, prefactors and whether or not to include the diffusion coefficient.

For completeness, this is the Usadel equation for the retared Green's function, $\hat{g}^R$. For the full Usadel equation in Keldysh space, we make the subsitution

$$\hat{g} \to \check{g} = \begin{pmatrix} \hat{g}^R & \hat{g}^K \\ 0 & \hat{g}^A \end{pmatrix}, \tag{2.30}$$

in eq. (2.29). We may relate the retared and advanced Green's functions by

$$\hat{g}^A = -\hat{\tau}_3 \left(\hat{g}^R\right)^\dagger \hat{\tau}_3, \tag{2.31}$$

and in equilibrium [37]

$$\hat{g}^K = \left(\hat{g}^R - \hat{g}^A\right) \tanh\left(\epsilon / 2k_B T\right). \tag{2.32}$$

As a final note it should be noted that the Usadel equation appear in the literature with $\hat{\Sigma} \to \epsilon\hat{\tau}_3 + \hat{\Sigma}$. This is more correct, as $\epsilon\hat{\tau}_3$ corresonds to the movement of a free quasielectron, while the self energy function encode the corrections to the movement. Collapsing the terms into a single matrix makes derivations less cluttered.

3 CURVED PROXIMITY SYSTEMS

The main focus of the thesis is curved superconductor-ferromagnet proximity systems. The purpose of this chapter is to more thoroughly motivate why we are considering these systems, and to present the necessary mathematical framework and notation to model these systems.

For superconductor-ferromagnet structures, curving the system comes with two consequences. First, the quasiparticle motion is confined to the material, and hence a curved path, and second that the curvature may alter the material properties. More specifically, we are concerned with the effects of constraining the quasiparticle movement to a spacecurve [38], how it interacts with the exchange field and the strain induced Rashba like spin orbit interaction [39, 40]. Before we consider the physics of such curved systems, we need the necessary mathematical tools and notation for describing space curves. This will be the parametrization of space curves, the arc length derivatives of these and the prerequisite tensor notation.

3.1 Tensor notation

In this section we introduce the covariant derivative, and the associated notation. As the subject matter is slightly outside that of a normal physics curriculum, it is a self contained introduction to the subject glossing over some of the subtleties. This section is loosely based on refs. [41, 42], where the former gives a thorough introduction to the subject.

VECTORS Given a vector space E with an inner product $\langle \cdot, \cdot \rangle$, we may represent any vector $\mathbf{V} \in E$ as a linear combination of a set of basis vectors, $\{\boldsymbol{e}_j\}$

$$\mathbf{V} = V^j \boldsymbol{e}_j. \tag{3.1}$$

Similarly, we may represent $\mathbf{V}$ by its projection onto the basis vectors – as is illustrated in fig. 3.1. This is typically done by writing

$$\mathbf{V} = V_j \boldsymbol{e}^j. \tag{3.2}$$

A more intuitive way may be to define $\{\boldsymbol{e}^j\}$ by

$$\boldsymbol{e}^j(\mathbf{V}) = V^j \tag{3.3}$$

That is, $\boldsymbol{e}^j$ is the linear functional that projects $\mathbf{V}$ onto $\boldsymbol{e}_j$. We may in turn make linear combinations of these functionals to represent $\mathbf{V}$. Note that this is strictly speaking not the vector itself, but the linear functional represented by $\langle \mathbf{V}, \cdot \rangle$, or the *covector* of $\mathbf{V}$. Accordingly, the basis (co)vectors are defined by

$$\boldsymbol{e}^j(\boldsymbol{e}_i) = \delta^j_i, \tag{3.4}$$

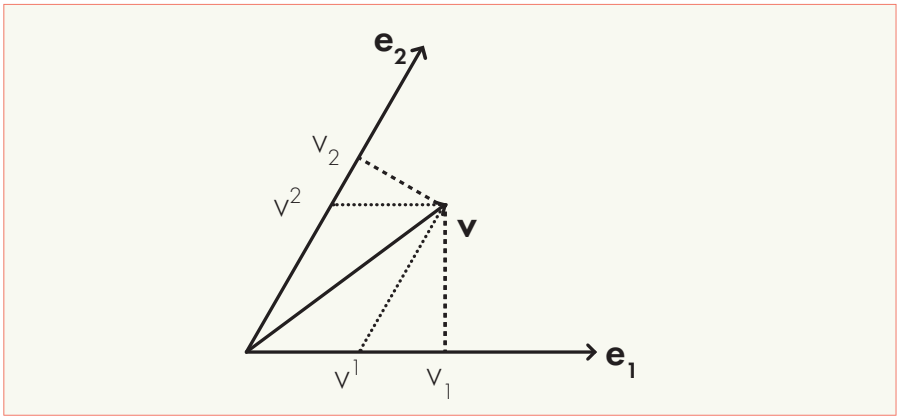

Figure 3.1: Given a set of basis vectors $\{\boldsymbol{e}_j\}$, we may determine a vector in terms of a linear combination of the basis vectors or the orthogonal projection onto each of the basis vectors. The former corresonds to the dotted lines, while the latter corresponds to the dashed lines.

and these are themselves linear functionals on E.

We refer to the coefficients, $\{V_i\}$ and $\{V^j\}$, as *covariant* and *contravariant* components respectively. The coefficients are related by

$$V_j = \sum_i V^i \eta_{ij}, \tag{3.5a}$$

$$V^i = \sum_j V_j \eta^{ij}, \tag{3.5b}$$

with

$$\eta = (\eta_{ij}), \quad \eta_{ij} = \langle \boldsymbol{e}_i, \boldsymbol{e}_j \rangle \tag{3.6a}$$

$$\eta^{-1} = (\eta^{ij}). \tag{3.6b}$$

We refer to η as the *metric tensor*, and η_{ij} as a *metric tensor element* [1]. With the inner product well defined, η is nondegenerate,[2] meaning it has an inverse.

TENSORS The notion of covariant and contravariant vectors may be generalized to that of *covariant* and *contravariant tensors*. A *covariant tensor* is a *multilinear* functional on tuples of vectors. We have already introduced the metric tensor, H. Written as a function on a tuple of vectors, we have

$$H(\boldsymbol{V}, \boldsymbol{W}) = \langle \boldsymbol{V}, \boldsymbol{W} \rangle = \sum_{ij} \eta_{ij} V^i W^j. \tag{3.7}$$

This is equivalent to some (square) matrix acting on $\boldsymbol{W}$. Observe that the function, i. e. H, is linear in both $\boldsymbol{V}$ and W. Similarly, a *contravariant tensor* is a multilinear function on tuples of covectors, with an example being the inverse of the metric tensor, H^{-1}.

We refer to the length of the tuple as the *rank* of the tensor, meaning H is a second rank covariant tensor.

---

1 Common symbols are G for the tensor, and g for its elements, but these are easiliy confused with the Green's functions.

2 We require $\langle \boldsymbol{v}, \boldsymbol{v} \rangle = ||\boldsymbol{v}|| = 0 \iff \boldsymbol{v} = 0$.

COVARIANT DERIVATIVE The idea of the *covariant derivative* is to extend the notion of the derivative, or rather, the gradient into a form that is independent of the choice of coordinate system.

For a more familiar example to build on, consider the derivative of a scalar function, $f(\underline{x})$, with respect to a vector $\boldsymbol{V}$[3], as such

$$\boldsymbol{V}(f(\underline{x})) = \langle \nabla f(\underline{x}), \boldsymbol{v} \rangle = \sum_j \frac{\partial f}{\partial x^j} v^j. \tag{3.8}$$

Here, $\underline{x}$ is a set of coordinates in some specific coordinate system $\{x^j\}$. Now, in exchanging the coordinate system, $\{x^j\}$, for a different coordinate system $\{z^j\}$, f, $\boldsymbol{V}$ and $\langle \nabla f, \boldsymbol{V} \rangle$ does not change

$$\frac{\partial f}{\partial z^j} = \sum_i \frac{\partial x^j}{\partial z^i} \frac{\partial f}{\partial x^j}. \tag{3.9}$$

This naturally extends to vectors, but not directly to their components. With $\boldsymbol{V} = V^i \boldsymbol{e}_i$, we have

$$\begin{aligned} \partial V^i &= \partial \left(\boldsymbol{e}^i \boldsymbol{V} \right) \\ &= \boldsymbol{e}^j \cdot (\partial \boldsymbol{V}) + \boldsymbol{V} \cdot \left(\partial \boldsymbol{e}^i \right). \end{aligned} \tag{3.10}$$

We may now define the *covariant derivative* (with respect to coordinate α) as

$$\begin{aligned} D_\alpha V^j &= \boldsymbol{e}^j \cdot (\partial_\alpha \boldsymbol{V}) \\ &= \partial_\alpha V^j - \boldsymbol{V} \cdot \left(\partial \boldsymbol{e}^i \right) \end{aligned} \tag{3.11}$$

The quantity should be understood as the projection of $\partial_\alpha \boldsymbol{V}$ onto $\boldsymbol{e}^j$.

Calculating the last term is however not trivial, but ∂_α is necessarily some linear combination of the chosen basis of covectors, $\{e^k\}$. Therefore, we write

$$\partial_i \boldsymbol{e}^j = -\Gamma^j_{ik} \boldsymbol{e}^k \tag{3.12}$$

such that we may rewrite eq. (3.11) as

$$D_i V^j = \partial_i V^j + \Gamma^j_{ik} V^k, \tag{3.13}$$

where we refer to the coefficients, Γ, as the *affine connection coefficients*[4].

It is possible to do something similar with the covariant components as well, where the (coordinate) covariant derivative is similar, but with different affine connection coefficients

$$\partial_i \boldsymbol{e}_j = \Gamma^k_{ji} \boldsymbol{e}_k, \tag{3.14a}$$

$$D_i V_j = \partial_i V_j - \Gamma^k_{ji} V_k. \tag{3.14b}$$

The choice of connection coefficients is not unique, here they are given as [42]

$$\Gamma^\mu_{\nu\lambda} = \frac{1}{2} \eta^{\mu\kappa} \left(\partial_\nu \eta_{\kappa\lambda} + \partial_\lambda \eta_{\nu\kappa} - \partial_\kappa \eta_{\nu\lambda} \right), \tag{3.15}$$

which allows us to evaluate the connection coefficients, Γ, and in turn the covariant derivatives for a particular system.

3 Here, $\underline{x}$ is some element in the domain of the function f, and should not be conflated with spin space or the inner product space we are considering, $E \ni V$.

4 The term *Christoffel symbols* is often used in the literature, or the terms are used interchangeably. The Christoffel symbols will be our particular choice affine connection coefficients.

3.2 Parametrization of curves in curvilinear coordinates

Consider a space curve, $\mathcal{C}$, parametrized by its arc length, s. That is, a function $\mathbf{r}(s)$ traces out $\mathcal{C}$. We may parametrize the neighbourhood, of $\mathcal{C}$, i. e. some open ball, by

$$\mathbf{R}(s, n, b) = \mathbf{r}(s) + n\hat{\mathrm{N}}(s) + b\hat{\mathrm{B}}(s), \tag{3.16}$$

where $\hat{\mathrm{N}}(s)$ and $\hat{\mathrm{B}}(s)$ are the basis vectors normal and binormal to the tangent vector of $\mathcal{C}$ at $\mathbf{r}(s)$, i. e. $\hat{\mathrm{T}}(s) = \partial_s \mathbf{r}(s)$.

Given a curve $\mathcal{C}$, we should be able to relate these vectors as a function of the arc length, s. We will employ the *Frenet-Serret* frame[5] [41, 43], with the derivation being similar to that of ref. [38].

The Frenet-Serret equations relate the basis vectors as such [43]

$$\begin{pmatrix} \partial_s \hat{\mathrm{T}}(s) \\ \partial_s \hat{\mathrm{N}}(s) \\ \partial_s \hat{\mathrm{B}}(s) \end{pmatrix} = \begin{pmatrix} 0 & \kappa(s) & 0 \\ -\kappa(s) & 0 & \tau(s) \\ 0 & -\tau(s) & 0 \end{pmatrix} \begin{pmatrix} \hat{\mathrm{T}}(s) \\ \hat{\mathrm{N}}(s) \\ \hat{\mathrm{B}}(s) \end{pmatrix}. \tag{3.17}$$

In one way, eq. (3.17) simply defines the arc length derivatives, but should rather be viewed as a way to encode the function $\mathbf{r}(s)$ into two scalar functions, $\kappa(s)$ and $\tau(s)$.

We will refer to $\kappa(s)$ as the *curvature*, or *curvature function*, and $\tau(s)$ as the *torsion* or *torsion function*. A simple picture is that the curvature function quantifies how non-straight the curve is, while the torsion quantifies how non-planar the curve is, with the plane in question being that spanned by the tangent and normal vector, $\hat{\mathrm{T}}$ and $\hat{\mathrm{N}}$. For a concrete example, a curve with zero torsion and constant curvature κ traces a circular arc with radius $1/\kappa$. If the torsion was non-zero, but constant, the curve would trace out a helix.

METRIC TENSOR The metric tensor is determined by $\kappa(s)$ and $\tau(s)$. Generally, we have [41]

$$\eta_{ij} = \left\langle \left(\frac{\partial \mathbf{p}}{\partial u^i}\right), \left(\frac{\partial \mathbf{p}}{\partial u^j}\right) \right\rangle, \tag{3.18}$$

where $\{\partial u^i\}$ are the basis vectors for some generalized coordinate system and $\mathbf{p}$ the point where we consider the derivatives. We may get the elements of the metric tensor, η_{ij}, by writing out the total derivatives and considering their products.

We start with the derivatives of $\mathbf{R}(s, n, b)$.

$$\begin{aligned} \left(\frac{\partial \mathbf{R}}{\partial s}\right) &= \frac{\partial \mathbf{r}(s)}{\partial s} + \frac{\partial}{\partial s}\left(n\hat{\mathrm{N}}(s)\right) + \frac{\partial}{\partial s}\left(b\hat{\mathrm{B}}(s)\right) \\ &= \hat{\mathrm{T}}(s) + n\left(-\kappa(s)\hat{\mathrm{T}}(s) + \tau(s)\hat{\mathrm{B}}(s)\right) + b\left(-\tau(s)\hat{\mathrm{N}}(s)\right) \\ &= \left(1 - n\cdot\kappa(s)\right)\hat{\mathrm{T}}(s) + n\cdot\tau(s)\hat{\mathrm{B}}(s) - b\cdot\tau(s)\hat{\mathrm{N}}(s), \end{aligned} \tag{3.19a}$$

$$\left(\frac{\partial \mathbf{R}}{\partial n}\right) = \frac{\partial \mathbf{r}(s)}{\partial n} + \frac{\partial}{\partial n}\left(n\hat{\mathrm{N}}(s)\right) + \frac{\partial}{\partial n}\left(b\hat{\mathrm{B}}(s)\right) \tag{3.20a}$$

$$= \hat{\mathrm{N}}(s), \tag{3.20b}$$

5 The name Serret-Frenet is also used in the literature

$$\left(\frac{\partial \mathbf{R}}{\partial n}\right) = \frac{\partial \mathbf{r}(s)}{\partial b} + \frac{\partial}{\partial b}\left(n\hat{N}(s)\right) + \frac{\partial}{\partial b}\left(b\hat{B}(s)\right) \tag{3.21a}$$

$$= \hat{B}(s). \tag{3.21b}$$

Explicitly, the elements of the metric tensor are thus given as

$$\eta_{ij} = \left(\frac{\partial \mathbf{R}}{\partial u^i}\right) \cdot \left(\frac{\partial \mathbf{R}}{\partial u^j}\right), \tag{3.22a}$$

with $\left\{\partial u^i\right\} = \{\partial s\, \partial n\, \partial b\}$. The full metric tensor is then given as

$$\begin{aligned}\eta &= (\eta_{ij}) \\ &= \begin{pmatrix} (1-n\cdot\kappa)^2 + \tau^2\cdot\left(n^2+b^2\right) & -b\cdot\tau & n\cdot\tau \\ -b\cdot\tau & 1 & 0 \\ n\cdot\tau & 0 & 1 \end{pmatrix},\end{aligned} \tag{3.23}$$

and its inverse as

$$\begin{aligned}\eta^{-1} = (\eta^{ij}) = \left(\frac{1}{1-n\cdot\kappa}\right)^2 \\ \cdot \begin{pmatrix} 1 & b\cdot\tau & -n\cdot\tau \\ b\cdot\tau & (b\cdot\tau)^2 + (\kappa\cdot n - 1)^2 & -bn\cdot\tau^2 \\ -n\cdot\tau & -bn\cdot\tau^2 & (n\cdot\tau)^2 + (\kappa\cdot n - 1)^2 \end{pmatrix},\end{aligned} \tag{3.24}$$

where both the curvature and torsion, κ, τ are still functions of the arc length, s.

The elements of the metric tensor are prerequisites for computing the affine connections, which we in turn need for the covariant derivatives of a spesific system. By eq. (3.15), we had

$$\Gamma^{\mu}_{\nu\lambda} = \frac{1}{2}\eta^{\mu\kappa}\left(\partial_\nu \eta_{\kappa\lambda} + \partial_\lambda \eta_{\nu\kappa} - \partial_\kappa \eta_{\nu\lambda}\right) \tag{3.25}$$

Note that with a symmetric[6] metric tensor, η_{ij}, the connection coefficient does not change if we permute the two lower indices. We will only be considering planar curves, meaning $\tau(s) = 0$, as that is sufficient for the physical phenomena we wish to consider in this thesis.

These expressions may simplify, depending on the choice of κ and τ. With $\tau(s) = 0$, the metric tensor turns diagonal, such that we may simplify eq. (3.25) with $\kappa \to \mu$

$$\Gamma^{\mu}_{\nu\lambda} = \frac{1}{2}\eta^{\mu\mu}\left(\partial_\nu \eta_{\mu\lambda} + \partial_\lambda \eta_{\nu\mu} - \partial_\mu \eta_{\nu\lambda}\right). \tag{3.26}$$

The non-zero affine connection coefficients are given as

$$\Gamma^{s}_{ss} = -\frac{n\cdot\kappa'}{1-n\cdot\kappa} = \frac{1}{H}\partial_s H, \tag{3.27a}$$

$$\Gamma^{n}_{ss} = \kappa - n\cdot\kappa^2 = -H\partial_n H, \tag{3.27b}$$

$$\Gamma^{s}_{sn} = \Gamma^{s}_{sn} = -\frac{\kappa}{1-n\cdot\kappa} = \frac{1}{H}\partial_n H. \tag{3.27c}$$

6 In more exotic contexts, the metric tensor does not have to be symmetric, e. g. in *nonsymmetric gravitational theory* [44].

with

$$H = H(s, n) = 1 - n \cdot \kappa(s). \tag{3.28}$$

The two last connection coefficients are equal, as the metric tensor is symmetric.

3.3 Effects of curvature on electronic systems

With the Frenet-Serret equations in place, we may consider the physical consequences of curvature. We will sketch how curvature induced strain may give rise to a spin orbit interaction, and how the Usadel equation and self energy terms changes when written in terms of arc-length derivatives. Notation conventions are inherited from refs. [45, 46] for easy reference.

CURVATURE AND SPIN-ORBIT COUPLING As a material is curved, it will strain – which in turn may give rise to spin orbit coupling. With the spin orbit coupling induced by the curvature, it is in principle both dynamic and tunable. We will, analogous to ref. [46], demonstrate how a spin orbit term would appear in the electron Hamiltonian.

The (engineering) strain, ϵ of a material is defined as its relative change in length [47]

$$\epsilon = \frac{L_{\text{final}} - L_{\text{initial}}}{L_{\text{initial}}} \tag{3.29}$$

where L is the length of the material. If the length increases we refer to the strain as *tensile*, and if the length decreases we refer to the strain as *compressive*. The picture complicates somewhat for non-isotropic systems, e. g. for some general crystal, in which case we may define the *strain tensor* [8] relating strained, $\boldsymbol{\nu}'_i$, and unstrained, $\boldsymbol{\nu}_i$ as such

$$\boldsymbol{\nu}'_i = \boldsymbol{\nu} + \epsilon_{ij}\boldsymbol{\nu}_j. \tag{3.30}$$

Observe the coefficients, ϵ_{ij} to be dimensionless. In the regime with *elastic strain* we are typically also assuming ϵ_{ij}^2 to be negligible.

Across a thin film, the strain in the tangential direction, ϵ_{ss}, is proportional to the curvature, $\kappa(s)$, and the depth at which we are considering the strain, i. e. n [48]. Explicitly,

$$\epsilon_{ss} = -n\frac{\partial^2 \zeta(s, b)}{\partial^2 s} = -n\kappa(s), \tag{3.31}$$

where $\zeta(s, b)$ is some surface within the film that is postulated to not strain, assumed to lay midway thorugh the film. With the strain continuous, such a surface must exist as the two surfaces have strain of opposite sign. The assumptions here are that the thickness of the film is small compared to the other dimensions of the film. This is the expression and explanation for the strain used in e. g. ref. [49].

We will however explicitly be considering curved nanowires, or *rods* in the language of ref. [48]. The expression does not immedeately translate to that of wires. In ref. [48], the authors consider a thin rod such that the axis of the

rod is colinear with, $\hat{z}$, and that there exist some *neutral surface* in the rod that does not strain when the rod is bent. Consider then some element of length dz a distance x form the neutral surface. If the rod is bent, the length changes to dz'. However, there is necessarily some unstrained element of equal length at the neutral surface that is by assumption bent but not strained. With the bending corresponding to a curvature of κ, the elements of length dz and dz' lay on circular arcs with radius $R = 1/\kappa$ and $R + x$. We may then relate dz and dz' by

$$dz' = \frac{R + x}{R} dz, \tag{3.32}$$

meaning the relative change in length, i. e. the strain, is given as

$$\epsilon_{zz} = \frac{dz' - dz}{dz} = \frac{x}{R} = x\kappa. \tag{3.33}$$

We may retrive eq. (3.31) with the substitution $z \to s$, $x \to -n$.

Note that the neutral surface is not, as was with the thin film, stated to be in the centre ofthe rod. Instead, ref. [48] argues that is at the (radial) centre of mass. While this might just seem like a curiosity, it is an assumption that may break down at the mesoscopic scale. There is of course also a *continuum* assumption here as well that could be discussed at length. In any case, a continuum in the radial direction does in some sense break down considering, e. g. hollow structures [50, 51].

Furthermore, the substitution $z \to s$ is also nontrivial; the arc length, s, relates explicitly to the length of the rod (segment). Therefore, the substitution comes with an additional assumption, namely that the arclength derivative is approximately equal to the derivative with respect to z. Another way of stating this is that the tangent vector, $\hat{T}$, is almost colinear with the z-axis at the point we are considering. As the strain gives rise to a *deformation potential* [7] [52],

$$V(s, n) = a\epsilon_{ss}(s, n) = -a\kappa(s)n, \tag{3.34}$$

where a is some proportionality constant This constant is some function of the bandstructure of the material in question, which in turn depends on the crystal structure, i. e. the strain. It should therefore be stressed that the assumption is that the potential is a linear function of the strain [52]. The assumption that the tangent vector $\hat{T}$ is almost colinear with the z-vector enters in assuming this expression for the deformation potential is only valid in the low-strain limit.

With a spatially varying potential, we must also have an electric field, with $\mathbf{E} = -\nabla V$. In the case with zero torsion, the electric field is given as [46]

$$\mathbf{E} = -\nabla V = \frac{a \cdot n}{1 - n \cdot \kappa(s)} \left(\partial_s \kappa(s)\right) \hat{T} + a \cdot \kappa(s) \hat{N}. \tag{3.35}$$

Assuming $n << 1/\kappa$, the left term is roughly porportional to n, and disappears if we average over the n-coordinatem resulting in

$$\langle \mathbf{E} \rangle_n = a\kappa(s)\hat{N}. \tag{3.36}$$

7 Note that we are assuming the other diagonal terms of the strain tensor ϵ can be neglected. It can be argued that the other diagonal terms of the *stress tensor* [48] are zero throughout the rod, which should be sufficient for a qualitative discussion,

As mentioned in the introduction, this corresponds to a magnetic field from the rest frame of a moving electron, and leads to a spin orbit coupling with strength proportional to the curvature function, κ.

INCLUDING SPIN ORBIT INTERACTIONS The spin orbit interaction can be included in the Usadel equation by means of the *spin orbit field*, $\underline{\mathbf{A}}$ [53, 54].

For a spin orbit coupling that is linear in momentum, the single particle Hamiltonian picks up a term like

$$H_{SO} = -\mathbf{p} \cdot \underline{\mathbf{A}}/2m. \tag{3.37}$$

The components of the spin orbit field, $\underline{\mathbf{A}} = \{\underline{A}_x, \underline{A}_y, \underline{A}_z\}$ are linear combinations of the Pauli matrices[8].

The spin orbit field will enter into the equations of motion by means of the *gauge covariant derivatives* [22], with

$$\nabla \cdot \to \tilde{\nabla} = \nabla \cdot - i\left[\hat{\mathbf{A}}, \cdot\right], \tag{3.38}$$

where $\hat{A} = \mathrm{diag}\,(\underline{A}, -\underline{A}^*)$. This can be motivated from reformulating the Hamiltonian with a spin-orbit term, and retracing the steps deriving the Usadel equation.

ARC LENGTH DERIVATIVES Similarly to how spin orbit interactions can be included in the Usadel equation by means of the gauge covatiant derivative, we transition to the Frenet-Serret frame with arc length derivatives by means of the coordinate covariate derivative, eq. (3.14a),

$$\nabla \boldsymbol{\nu} = \partial_i \nu_i \to D_i \nu_i = \partial_i \nu_i - \Gamma^k_{ji} \nu_k. \tag{3.39}$$

If we wish to include spin orbit interactions as well, we exchange the "ordinary" gradient operator with the gauge covariant derivative – this will be the coordinate gauge covariant derivative. The focus of chapter 4 is to write explicit forms of the Usadel equation in terms of the gauge covariant derivative.

In ref. [46], the system Hamiltonian including spin orbit interaction, is reformulatied in the covariant form and tuned to a curved 1D wire by "[...] *including a constraining potential in the normal and binormal directions*". The final result is the Hamiltonian [38, 46]

$$\begin{aligned} H = &-\frac{\hbar}{2m}\left[\partial_s^2 + \frac{\kappa^2}{4} + \frac{\tau^2}{2}\right] \\ &- i\hbar\alpha_N\left[\underline{\sigma}_B \partial_s - \underline{\sigma}_N \frac{\tau}{2}\right] \\ &+ i\hbar\alpha_B\left[\underline{\sigma}_N \partial_s - \underline{\sigma}_T \frac{\kappa}{2} + \underline{\sigma}_B \frac{\tau}{2}\right], \end{aligned} \tag{3.40}$$

where we have re-added the torsion dependent terms form [38]. For clarity, $\underline{\sigma}_{\{T,N,B\}} = \underline{\sigma} \cdot \{\hat{T}, \hat{N}, \hat{B}\}$, are the Pauli matrices in the Frenet-Serret frame, and α are coefficients determining the spin-orbit field strength. Here, only the momentum along the tangential direction couples to the spin, corresponding to the spin orbit field[38, 46]

$$\underline{\mathbf{A}} = (\alpha_N \sigma_B - \alpha_B \sigma_N, 0, 0). \tag{3.41}$$

8 In ref. [53], the factor $\frac{1}{2}$ in the denominator is accounted for by scaling the Pauli matrices.

As mentioned, the curvature induced spin orbit interaction is along the normal direction, correspond to α_N. Rederiving the Usadel equation from his Hamiltonian is equivalent to replacing the gradient operators with their gauge-coordinate covariant counterparts.

EXCHANGE FIELD IN CURVILINEAR COORDINATES In Cartesian coordinates, we were able to postulate an exchange field, $\mathbf{h}$, with components along the x, y and z axes. The corresponding self energy term is [55]

$$\hat{\Sigma}_{FM} = \mathbf{h} \cdot \hat{\boldsymbol{\sigma}}, \tag{3.42}$$

with $\hat{\boldsymbol{\sigma}} = \text{diag}\,(\underline{\sigma}, \underline{\sigma}^*)$. This corresponding to the spin-splitting of the energy levels, with the electron energy shifting by $\mathbf{h} \cdot \underline{\sigma}$. We transform the term to the Frenet-Serret frame by writing the dot product in terms of the metric tensor,

$$\hat{\Sigma}_{FM} = \eta^{ij} h_i \hat{\sigma}_j. \tag{3.43}$$

Raising this self energy term to Keldysh space is done by a Kronecker product with a 2×2 identity matrix.

Additionally, we will be assuming that the exchange field is colinear with the tangent vector, $\mathbf{h} \parallel \hat{\mathbf{T}}$. The deviations are in ref. [45] assumed negligible until the local curvature function reaches some critical value [56]. The Pauli matrices will however be functions of the curvature, such that the self energy term undergoes a rotation in spin space. From the symmetry of the inner product, this equivalent to having a rotating exchange field and fixed Pauli matrices [45].

SUPERCONDUCTING ORDER For completenes, we should also consider the effect of curvature on the superconducting order. Spesific to this thesis, this is a rather mundane consideration, as we are not considering curved superconducting regions, and the regions we are considering are assumed to be bulk regions of conventionals-wave BCS superconductors. Thus, the superconducting gap undergoes the rather trivial transformation

$$\Delta(x, y, z) \to \Delta(s, n, b) = \Delta, \tag{3.44}$$

which does not alter the contribution of the superconducting order to the self energy function

$$\hat{\Sigma}_{SC} = \hat{\Delta} = \text{antidiag}\,(-\Delta^*, \Delta^*, -\Delta, \Delta)\,, \tag{3.45}$$

where Δ is the superconducting gap, and we are subscribing to the convention of having the antidiagonal run from the bottom left corner to the top right. Raising this self energy term to Keldysh space is done by a Kronecker product with a 2×2 identity matrix.

However, as a sidenote, the superconducting gap is expected to obey a *self consistency equation* [57], which for our system with straight superconducting regions trivially transforms to curvilinear coordinates [46]. This picture may complicate in the presence of curved superconducting regions or with a superconducting order parameter with a different type of symmetry [58] or effects relating to the finite size, or reduced dimentionality of the superconductor [59].

VALIDITY OF THE USADEL EQUATION In deriving the Usadel equation, we made the assumption that the self energy terms, or rather the perturbations to the system Hamiltonian, vary slowly compared to the Fermi wavelength — this was for the quasiclassical approximation — as well as the scattering potential being only a function of the direction of the momentum, and not position. This places limits on, at least, the spatial variations of the deformation potential of eq. (3.34) and the deformation of the material should not impact the spatial distribution of impurities to scatter of.

Furthermore, the treatment of strains in ref. [8] assumes the strain to be infinitesimal, as well as being applied isothemally or adiabatically. As we will not explicitly consider strained structures, this bears little direct relevance on our calculations, but could be important considerations in systems where the curvature is changed dynamically.

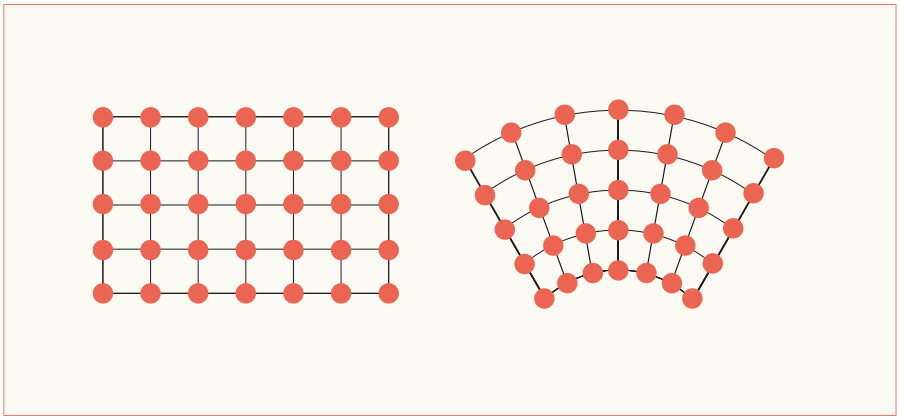

Figure 3.2: Schematic of a unstrained (left) and strained (right) wire. The top of the wire experiences tensile strain in the tangential direction, with the density of atoms along the wire being lower than in the unstrained case. The bottom of the wire experiences compressive strain in the tangenial direction, with the density of atoms higher than in the unstrained case. With the assumption that the strain varies continuously, there must exist some unstrained plane inside the wire.

4 THE USADEL EQUATION IN CURVED SYSTEMS

In chapter 2, we had the *Usadel equation*, eq. (2.29), written as

$$D_F \nabla (\check{g} \nabla \check{g}) = -i \left[\check{\Sigma}, \check{g}\right], \tag{4.1}$$

where $\check{g}$ is the quasiclassical (isotropic) Green's function, D_F the diffusion constant and $\check{\Sigma}$ the self-energy function in Keldysh space. Considering only (s-wave) superconducting and ferromagnetic order, raising the Usadel equation from Nambu⊗spin to Keldysh space is done by raising the relevant terms to Keldysh space [60], i. e. $\check{\Sigma} = \operatorname{diag}\left(\hat{\Sigma}, \hat{\Sigma}\right)$. Again, for compactness, the term $\epsilon\hat{\tau}_3$ is included in the self energy function.

In this chapter we will rewrite the Usadel equation in an explicit form in terms of the arc legnth derivative, ∂_s, for a 1D nanowire. This will be the full equation, which trivialy transforms to equations for the equilibrium propagators, $\hat{g}^R$ and $\hat{g}^A$, as well as a quantum kinetic equation that allows us to determine $\hat{g}^K$ and in turn non-equilibrium properties of the system.

4.1 Including arc-length derivatives

We may rewrite the Usadel equation in curvilinear coordinates as such

$$iD_F \eta^{ij} D_i \left(\check{g} D_j \check{g}\right) = \left[\check{\Sigma}, \check{g}\right]. \tag{4.2}$$

Where the the gradient operator is replaced with covarient derivatives of section 3.1 and the inner products are written in terms of the metric tensor, $\eta = (\eta_{ij})$.

To solve the Usadel equation, we will need it in some tractable form, i. e. written out explicitly with differentiation operators and coefficients, we start my writing out the coordinate covariant derivatives, eq. (3.14a),

$$D_i \nu_k = \partial_i \nu_k - \Gamma^j_{ik} \nu_k. \tag{4.3}$$

To get the Usadel equation in a tractable form, we will need to write explicit forms of the affine connection coefficients. With the motion constrained along a 1D wire without torsion, we had from eq. (3.27)

$$\Gamma^s_{ss} = -\frac{n \cdot \kappa'}{1 - n \cdot \kappa} = \frac{1}{H}\partial_s H, \tag{4.4a}$$

$$\Gamma^n_{ss} = \kappa - n \cdot \kappa^2 = -H\partial_n H, \tag{4.4b}$$

$$\Gamma^s_{sn} = \Gamma^s_{sn} = -\frac{\kappa}{1 - n \cdot \kappa} = \frac{1}{H}\partial_n H. \tag{4.4c}$$

with

$$H = H(s, n) = 1 - n \cdot \kappa(s). \tag{4.5}$$

Supressing the scalar prefactors, the left hand side of the Usadel equation is given as

$$
\begin{aligned}
&\eta^{ij} D_i \left(\check{g} D_j \check{g}\right) \\
&= \eta^{ij} D_i \left(\check{g} \partial_j \check{g}\right) \\
&= \eta^{ij} \left[\partial_i \left(\check{g} \partial_j \check{g}\right) - \Gamma^k_{ij} \left(\check{g} \partial_k \check{g}\right)\right], \\
&= \eta^{jj} \left[\partial_j \left(\check{g} \partial_j \check{g}\right) - \Gamma^k_{jj} \left(\check{g} \partial_k \check{g}\right)\right], \qquad \eta^{ij} = 0 \text{ for } i \neq j \\
&= \eta^{ss} \left[\partial_s \left(\check{g} \partial_s \check{g}\right) - \Gamma^s_{ss} \left(\check{g} \partial_s \check{g}\right) - \Gamma^n_{ss} \left(\check{g} \partial_s \check{g}\right)\right] \\
&\quad + \eta^{nn} \left[\partial_n \left(\check{g} \partial_n \check{g}\right) + 0\right], \qquad \Gamma^n_{jj} = 0 \text{ for } j \neq s \\
&\quad + \eta^{bb} \left[\partial_b \left(\check{g} \partial_b \check{g}\right) + 0\right], \qquad \Gamma^b_{jj} = 0 \\
&= H^{-2} \left[\partial_s \left(\check{g} \partial_s \check{g}\right) - H^{-1} \partial_s H \cdot \left(\check{g} \partial_s \check{g}\right)\right. \\
&\quad \left. + H \partial_n H \cdot \left(\check{g} \partial_n \check{g}\right)\right] \\
&\quad + \left[\partial_n \left(\check{g} \partial_n \check{g}\right) + \partial_b \left(\check{g} \partial_b \check{g}\right)\right].
\end{aligned} \tag{4.6}
$$

To further simplify the expression, we calculate some intermediary quantities. We have

$$
\begin{aligned}
&H^{-2} \left[\left(\check{g} \partial_s \check{g}\right) + H^{-1} \partial_s H \left(\check{g} \partial_s \check{g}\right)\right] \\
&= H^{-1} \left[H^{-1} \left(\check{g} \partial_s \check{g}\right) + H^{-2} \partial_s H \left(\check{g} \partial_s \check{g}\right)\right] \\
&= H^{-1} \partial_s \left(H^{-1} \check{g} \partial_s \check{g}\right),
\end{aligned} \tag{4.7}
$$

and

$$
\begin{aligned}
&H^{-2} H (\partial_n H) \left(\check{g} \partial_n \check{g}\right) + \partial_n \left(\check{g} \partial_n \check{g}\right) \\
&= H^{-1} \left[\partial_n H \left(\check{g} \partial_n \check{g}\right) + H \partial_n \left(\check{g} \partial_n \check{g}\right)\right] \\
&= H^{-1} \partial_n \left(H \check{g} \partial_n \check{g}\right).
\end{aligned} \tag{4.8}
$$

Inserting these back into eq. (4.6) gives

$$
\begin{aligned}
\eta^{ij} D_i \left(\check{g} D_j \check{g}\right) = {} & H^{-1} \partial_s \left(H^{-1} \check{g} \partial_s \check{g}\right) \\
& + H^{-1} \partial_n \left(H \check{g} \partial_n \check{g}\right) + \partial_b \left(\check{g} \partial_b \check{g}\right).
\end{aligned} \tag{4.9}
$$

This is an explicit form of the Usadel equation for a region close to a planar curve that only depends on $\kappa(s)$. For completeness, the full Usadel equation then becomes

$$
i D_F \left\{H^{-1} \partial_s \left(H^{-1} \check{g} \partial_s \check{g}\right) + H^{-1} \partial_n \left(H \check{g} \partial_n \check{g}\right) + \partial_b \left(\check{g} \partial_b \check{g}\right)\right\} = \left[\check{\Sigma}, \check{g}\right]. \tag{4.10}
$$

Explicitly limiting the quasiparticle movement to the curve, we ignore the ∂_n and ∂_b terms, as well as having $n = b = 0$, such that $H = 1$. In that case eq. (4.9) simplifies to

$$
\eta^{ij} D_i \left(\check{g} D_j \check{g}\right) = \partial_s \left(\check{g} \partial_s \check{g}\right), \tag{4.11}
$$

with the full form being

$$
i D_F \partial_s \left(\check{g} \partial_s \check{g}\right) = \left[\Sigma, \check{g}\right]. \tag{4.12}
$$

Note that, compared to eq. (4.1), there are no explicit changes. The curvature manifests in that the self-energy terms are written in the Frenet-Serret frame, rather than the xyz-frame. This holds for any (continuously differentiable) choice of curvature function, $\kappa(s)$.

4.2 Including Spin-Orbit Coupling

We include spin-obit coupling by exchanging the coordinate-covariant derivatives with the *coordinate-gauge covariant derivatives* [46], meaning

$$D_i v^j = \partial_i v_j - \Gamma^k_{ij} v_k \to \tilde{D}_i v^j = \partial_i v_j - \Gamma^k_{ij} v_k - i\left[\hat{A}_i, v_j\right], \tag{4.13}$$

where $\hat{A}_i = \mathrm{diag}(\underline{A}_i, -\underline{A}_i^*)$ is the covariant spin-orbit field in Nambu $\otimes$ spin space [22, 53] — it is promoted to Keldysh space with a simple Kronecker product with a 2×2 identity matrix. In this section, we rederive the Usadel equation with non-zero spin-orbit fields, analogous to a derivation carried out in ref. [46]

Consider first,

$$\begin{aligned} \check{g}\tilde{D}_j\check{g} &= \check{g}\left(D_j\check{g} - i\left[\hat{A}_j, \check{g}\right]\right) && (4.14a)\\ &= \check{g}D_j\check{g} - i\check{g}\left[\hat{A}_j, \check{g}\right]. && (4.14b)\end{aligned}$$

And then what is essentially the full left hand side of the Usadel equation

$$\begin{aligned} \tilde{D}_i\check{g}\tilde{D}_j\check{g} =& \tilde{D}_i\check{g}D_j\check{g} - i\tilde{D}_i\check{g}\left[\hat{A}_j, \check{g}\right] && (4.15a)\\ =& D_i\check{g}D_j\check{g} - i\left[\hat{A}_i, \check{g}D_j\check{g}\right] && (4.15b)\\ & - i\left(D_i\check{g}\left[\hat{A}_j, \check{g}\right] - i\left[\hat{A}_i, \check{g}\left[\hat{A}_j, \check{g}\right]\right]\right). \end{aligned}$$

With $D_j \to \nabla$, we will retrive the Usadel equation in Cartesian coordinates with a spin-orbit field [57].

Writing out the above explicitly in terms of the derivatives and connection coefficients will for each term in eq. (4.15b) give

$$\begin{aligned} D_i\check{g}D_j\check{g} &= D_i\check{g}\partial_j\check{g} && (4.16a)\\ &= \partial_i\check{g}\partial_j\check{g} - \Gamma^k_{ij}\check{g}\partial_j\check{g}, && (4.16b)\\ -i\left[\hat{A}_i, \check{g}D_j\check{g}\right] &= -i\left[\hat{A}_i, \check{g}\partial_j\check{g}\right], && (4.16c)\\ -iD_i\check{g}\left[\hat{A}_j, \check{g}\right] &= -i\partial_i\left(\check{g}\left[\hat{A}_j, \check{g}\right]\right) + i\Gamma^k_{ij}\left[\hat{A}_k, \check{g}\right], && (4.16d)\end{aligned}$$

where we in the third line interchanged the indices to arrive at a more readable final result. Combining these, we arrive at

$$\begin{aligned} \tilde{D}_i\check{g}\tilde{D}_j =& \partial_i\left(\check{g}\partial_j\check{g}\right) - \Gamma^k_{ij}\check{g}\partial_j\check{g}\\ & - i\left[\hat{A}_j, \check{g}\partial_i\check{g}\right] - i\partial_i\left(\check{g}\left[\hat{A}_j, \check{g}\right]\right)\\ & + i\Gamma^k_{ij}\check{g}\left[\hat{A}_k, \check{g}\right] - \left[\hat{A}_i, \check{g}\left[\hat{A}_j, \check{g}\right]\right] \end{aligned} \tag{4.17}$$

The next step is to evaluate the connection coefficients. While the above does not depend on the choice of curvature and torsion functions, κ and τ, we will again limit ourselves to a system without torsion. From eq. (4.9), we already have the first two terms evaluated, with

$$\begin{aligned} &\eta^{ij}\left(\partial_i\left(\check{g}\partial_j\check{g}\right) - \Gamma^k_{ij}\check{g}\partial_j\check{g}\right)\\ &= H^{-1}\partial_s\left(H^{-1}\check{g}\partial_s\check{g}\right)\\ &+ H^{-1}\partial_n\left(H\check{g}\partial_n\check{g}\right) + \partial_b\left(\check{g}\partial_b\check{g}\right). \end{aligned} \tag{4.18}$$

For the two terms involving "non-trivial" derivatives, we have

$$\begin{aligned}
&\eta^{ij}\Big\{-i\partial_i\left(\check{g}\left[\hat{A}_j,\check{g}\right]\right)+i\Gamma^k_{ij}\check{g}\left[\hat{A}_k,\check{g}\right]\Big\}\\
&=-\frac{i}{H}\partial_s\left(\frac{1}{H}\left(\check{g}\hat{A}_s\check{g}-\hat{A}_s\right)\right)\\
&\quad-iH\partial_n\left(\frac{1}{H}\left(\check{g}\hat{A}_n\check{g}-\hat{A}_n\right)\right)\\
&\quad-i\left(\partial_b\check{g}\right)\hat{A}_b\check{g}-\check{g}\hat{A}_b\partial_b\check{g}.
\end{aligned}\tag{4.19}$$

Note that we have assumed $A_{s,n,b}$ to be constant, and used that the metric tensor is diagonal, such that $j\to i$. For the final two terms we have

$$\begin{aligned}
&\eta^{ij}\left\{-i\left[\hat{A}_i,\check{g}\partial_j\check{g}\right]-\left[\hat{A}_i,\check{g}\left[\hat{A}_j,\check{g}\right]\right]\right\}\\
&=\frac{1}{H}\left(-i\left[\hat{A}_s,\check{g}\partial_s\check{g}\right]-\left[\hat{A}_s,\check{g}\left[\hat{A}_s,\check{g}\right]\right]\right)\\
&\quad+\left(-i\left[\hat{A}_n,\check{g}\partial_n\check{g}\right]-\left[\hat{A}_n,\check{g}\left[\hat{A}_n,\check{g}\right]\right]\right)\\
&\quad+\left(-i\left[\hat{A}_b,\check{g}\partial_b\check{g}\right]-\left[\hat{A}_b,\check{g}\left[\hat{A}_b,\check{g}\right]\right]\right)
\end{aligned}\tag{4.20}$$

Analogous to what we did without spin orbit coupling, the equation simplifies with $H=1-n\kappa(s)\to 1$ and we may supress the ∂_n and ∂_b terms. In that case, the full Usadel equation becomes

$$iD_F\Big\{\partial_s\left(\check{g}\partial_s\check{g}\right)-i\partial_s\left(\check{g}\hat{A}_s\check{g}\right)-i\left[\hat{A}_s,\check{g}\partial_s\check{g}\right]-\left[\hat{A}_k,\check{g}\left[\hat{A}_k,\check{g}\right]\right]\Big\}=\left[\check{\Sigma},\check{g}\right],\tag{4.21}$$

where $\hat{A}_k=\left\{\hat{A}_s,\hat{A}_n,\hat{A}_b\right\}$. Again, this equation looks as the one in Cartesian coordinates, but it should be noted that the self-energy matrix, Σ, is written in the curvilinear coordinates.

4.3 Boundary conditions

As mentioned in section 2.2, we are assuming the quasiclassical Green's function to vary slowly compared to the length-scales of the physical system. This assumption breaks down at interfaces, and there are several choices for boundary conditions to resolve this.

TRANSPARENT BOUNDARY CONDITIONS The most naive choice of boundary conditions is that of transparent boundary conditions, meaning we require

$$\check{g}_L=\check{g}_R,\tag{4.22}$$

with L,R denoting the Green's function on the left and right side of the interface. We will use these boundary conditions briefly in looking at normal metal - normal metal interfaces out of equilibrium.

KUPRIYANOV -LUKICHEV BOUNDARY CONDITIONS We will use the *Kupriyanov -Lukichev* boundary conditions [61] here given as

$$\check{g}_nD_i\check{g}_n=\frac{1}{2L_n\zeta_n}\left[\check{g}_L,\check{g}_R\right],\tag{4.23}$$

where n is an index denoting one side of the interface, L_n is the length of said region and ζ_n the ratio of the interface resistance to the bulk resistance of the region n. This particular formulation is adapted from [57].

Written explicitly with a non-zero spin-orbit field for our one dimensional systems, we get [57]

$$\check{g}_j \partial_s \check{g}_i = \frac{1}{2L_i\zeta_i}\left[\check{g}_L, \check{g}_R\right] + i\check{g}_i\left[\hat{A}_z, \check{g}_i\right] \tag{4.24}$$

For the Riccati parametrization, the derivation is presented in ref. [57], but for real spin-orbit fields. We restate the (general) end result as

$$\partial_s\gamma_L = \frac{1}{L_L\zeta_L}\left(1-\gamma_L\tilde{\gamma}_R\right)N_R\left(\gamma_R-\gamma_L\right) + i\hat{A}_s\gamma_L + i\gamma_L\hat{A}_s^*, \tag{4.25a}$$

$$\partial_s\gamma_R = \frac{1}{L_R\zeta_R}\left(1-\gamma_R\tilde{\gamma}_L\right)N_L\left(\gamma_R-\gamma_L\right) + i\hat{A}_s\gamma_R + i\gamma_R\hat{A}_s^*. \tag{4.25b}$$

We may of course apply the $\tilde{\cdot}$ conjugation to the above expressions to get boundary conditions for $\tilde{\gamma}$.

Note how in section 2.3, we had written the non-isotropic part of the Green's function as

$$\check{g}_p = D_F\check{g}_s\nabla_{\mathbf{R}}\check{g}_s, \tag{4.26}$$

where we compared to eq. (2.26) have written the expression in Keldysh space, rather than Nambu⊗spin space. The Kupriyanov -Lukichev does, as we have stated them here, estimate the tunneling probability of the *matrix current* $\check{g}_p$.

It should be noted that more general boundary conditions exist. These are suitable to incorporate effects like spin active interfaces, and contributions from reflection as well as tunneling [62].

4.4 Keldysh Component

Looking at the whole Usadel equation, there is some redundancy. Given the retarded component, $\hat{g}^R$, we may find the advanced component $\hat{g}^A = -\hat{\tau}_3\left(\hat{g}^R\right)^\dagger\hat{\tau}_3$ [31]. For the Keldysh component, $\hat{g}^K$, the picture is slightly more complicated. We do however have the ansatz [27]

$$\hat{g}^K = \hat{g}^R\hat{h} - \hat{h}\hat{g}^A, \tag{4.27}$$

where we refer to $\hat{h}$ as the *distribution matrix*. With this ansatz, and the normalization condition $\hat{g}^R\hat{g}^R = \hat{g}^A\hat{g}^A = 1$, we also achieve $\check{g}\check{g} = 1$ as was mentioned in section 2.2. The choice of $\hat{h}$ is however not uniquely defined [35], even though $\hat{g}^K$ is for a given $\hat{g}^A$ and $\hat{g}^R$.

With this ansatz for the Keldysh component, it is in principle sufficient to derive equations explicitly for $\hat{g}^R$ and $\hat{h}$ to fully describe a system We will see that the equation for $\hat{g}^R$ does not depend on $\hat{h}$ — meaning we may first solve the Usadel equation for $\hat{g}^R$ and then for $\hat{h}$. This picture does however complicate if we need to solve the Usadel equation self-consistently for the superconducting gap Δ.

To solve the equation for the distribution matrix, $\hat{h}$, numerically, we will be employing a scheme decomposing the distribution matrix in (block) diagonal

Nambu(⊗spin) space. The notation is inherited from ref. [60], but similar approaches are used in e. g. [31, 63].

PARAMETRIZATION OF THE DISTRIBUTION MATRIX We start by assuming the distribution matrix to be diagonal in Nambu space [] which is a valid assumption at low frequencies [31, 64]. We may then decompose the distribution matrix, h, in terms of a set of basis matrices spanning the block diagonal Nambu⊗spin space as such

$$\hat{h} = h_n \hat{\rho}_n, \tag{4.28}$$

with

$$\hat{\rho}_{0,1,2,3} = \hat{\tau}_0 \hat{\sigma}_{0,1,2,3}, \tag{4.29a}$$
$$\hat{\rho}_{4,5,6,7} = \hat{\tau}_3 \hat{\sigma}_{0,1,2,3}, \tag{4.29b}$$
$$\hat{\tau}_0 = I_4, \quad \hat{\tau}_3 = \mathrm{diag}\,(1,1,-1,-1) \tag{4.29c}$$
$$\hat{\sigma}_j = \mathrm{diag}\left(\underline{\sigma}_j, \underline{\sigma}_j^*\right). \tag{4.29d}$$

We may determine the coefficients, h_n, from traces with the basis matrices as such

$$h_n = \frac{1}{4}\mathrm{Tr}\left\{\hat{\rho}_n \hat{h}\right\}. \tag{4.30}$$

As we have selected a real vector space with a real field of scalars,we may the treat $\{h_m\}$ as a real vector of length 8.

Starting from eq. (4.21), we may rewrite the full Usadel equation for our 1D wire as

$$D_F\left\{\tilde{\partial}_s\left(\check{g}\tilde{\partial}_s\check{g}\right)\right\} = -i\left[\check{\Sigma}, \check{g}\right], \tag{4.31}$$

where we compared to eq. (4.21) have written the equation in terms of a gauge covariant arc length derivative. We may write the equation even more compactly in terms of the gauge covariant *matrix current*

$$\tilde{\partial}_s \check{I} = -i\left[\check{\Sigma}, \check{g}\right], \tag{4.32}$$

with

$$\check{I} = D_F\left(\check{g}\tilde{\partial}_s\check{g}\right). \tag{4.33}$$

To arrive at an equation for the matrix current, we may apply the parametrization of the distribution matrix to the Keldysh component of these two equations, differentiate the latter and set them equal to each other. We start with the matrix current,

$$\begin{aligned}\check{I} =& D_F\left(\check{g}\tilde{\partial}_s\check{g}\right)\\ =& D_F\left(\check{g}\partial_s\check{g}\right) - iD_F\check{g}\left[\hat{\mathbf{A}}, \check{g}\right]\\ =& D_F\left(\check{g}\partial_s\check{g}\right) - iD_F\left(\check{g}\hat{\mathbf{A}}\check{g} - \hat{\mathbf{A}}\right)\end{aligned} \tag{4.34}$$

with the Keldysh component

$$\begin{aligned}\hat{I}^K =& D_F\left\{\left(\hat{g}^R\partial_s\hat{g}^R\right)\hat{h} - \hat{h}\left(\hat{g}^A\partial_s\hat{g}^A\right)\right\}\\ &+ D_F\left\{\partial_s\hat{h} - \hat{g}^R\left(\partial_s\hat{h}\right)\hat{g}^A\right\}\\ &- iD_F\left\{\hat{g}^R\hat{\mathbf{A}}\hat{g}^R\hat{h} - \hat{h}\hat{g}^A\hat{\mathbf{A}}\hat{g}^A\right\}.\end{aligned} \tag{4.35}$$

We now make the substitution $\hat{h} \to \hat{\rho}_m h_m$

$$\begin{aligned}\hat{I}^K =& D_F \left\{ \left(\hat{g}^R \partial_s \hat{g}^R \right) \hat{\rho}_m - \hat{\rho}_m \left(\hat{g}^A \partial_s \hat{g}^A \right) \right\} h_m \\ &+ D_F \left\{ \hat{\rho}_m - \hat{g}^R \hat{\rho}_m \hat{g}^A \right\} \partial_s h_m \\ &- i D_F \left\{ \hat{g}^R \hat{\mathbf{A}} \hat{g}^R \hat{\rho}_m - \hat{\rho}_m \hat{g}^A \hat{\mathbf{A}} \hat{g}^A \right\} h_m. \end{aligned} \tag{4.36}$$

The next step is mulitplying from the left with $\hat{\rho}_n$, taking the trace and mulitplying by $1/4$ and introducing

$$I_n = \frac{1}{4} \mathrm{Tr} \left\{ \hat{\rho}_n \hat{I}^K \right\}. \tag{4.37}$$

Then, eq. (4.36) becomes

$$\begin{aligned} I_n =& \frac{D_F}{4} \mathrm{Tr} \left\{ \left(\hat{\rho}_n \hat{g}^R \partial_s \hat{g}^R \right) \hat{\rho}_m - \hat{\rho}_n \hat{\rho}_m \left(\hat{g}^A \partial_s \hat{g}^A \right) \right\} h_m \\ &+ \frac{D_F}{4} \mathrm{Tr} \left\{ \hat{\rho}_n \hat{\rho}_m - \hat{\rho}_n \hat{g}^R \hat{\rho}_m \hat{g}^A \right\} \partial_s h_m \\ &- \frac{i D_F}{4} \mathrm{Tr} \left\{ \hat{\rho}_n \hat{g}^R \hat{\mathbf{A}} \hat{g}^R \hat{\rho}_m - \hat{\rho}_n \hat{\rho}_m \hat{g}^A \hat{\mathbf{A}} \hat{g}^A \right\} h_m. \end{aligned} \tag{4.38}$$

Note that the entries of the traces are permuted in ref. [60]. We may write this more compactly as

$$I_n = Q_{nm} h_m + M_{nm} \partial_s h_m - i S_{nm} h_m, \tag{4.39a}$$

$$Q_{nm} = \frac{D_F}{4} \mathrm{Tr} \left\{ \hat{\rho}_n \hat{g}^R \partial_s \hat{g}^R \hat{\rho}_m - \hat{\rho}_n \hat{\rho}_m \hat{g}^A \partial_s \hat{g}^A \right\} h_m \tag{4.39b}$$

$$M_{nm} = \frac{D_F}{4} \mathrm{Tr} \left\{ \hat{\rho}_n \hat{\rho}_m - \hat{\rho}_n \hat{g}^R \hat{\rho}_m \hat{g}^A \right\} \tag{4.39c}$$

$$S_{nm} = \frac{D_F}{4} \mathrm{Tr} \left\{ \hat{\rho}_n \hat{g}^R \hat{\mathbf{A}} \hat{g}^R \hat{\rho}_m - \hat{\rho}_n \hat{\rho}_m \hat{g}^A \hat{\mathbf{A}} \hat{g}^A \right\}. \tag{4.39d}$$

Returning to the Usadel equation itself, we may apply the parametrization to the right hand side with

$$\begin{aligned} \left\{ -i \left[\check{\Sigma}, \check{g} \right] \right\}^K &= -i \left[\hat{\Sigma}, \hat{g}^K \right] \\ &\to -\frac{i}{4} \mathrm{Tr} \left\{ \hat{\rho}_n \left[\hat{\Sigma}, \left(\hat{g}^R \hat{\rho}_m - \hat{\rho}_m \hat{g}^A \right) \right] \right\} h_m \\ &= -V_{nm} h_m, \end{aligned} \tag{4.40}$$

where we have used $\hat{g}^K \to \left(\hat{g}^R \hat{\rho}_m - \hat{\rho}_m \hat{g}^A \right) h_m$ and introduced the shorthand

$$V_{nm} = \frac{i}{4} \mathrm{Tr} \left\{ \hat{\rho}_n \left[\hat{\Sigma}, \left(\hat{g}^R \hat{\rho}_m - \hat{\rho}_m \hat{g}^A \right) \right] \right\}. \tag{4.41}$$

For the left hand side of the Usadel equation, we have

$$\tilde{\partial}_s \check{I} = \partial_s \check{I} - i \left[\hat{\mathbf{A}}, \check{I} \right], \tag{4.42}$$

meaning we may write the arc length derivative of the matrix current as

$$\partial_s \check{I} = -i \left[\hat{\mathbf{A}}, \check{I} \right] + i \left[\hat{\mathbf{A}}, \check{I} \right]. \tag{4.43}$$

We are however interested in the Keldysh component; and consider first the last term

$$\begin{aligned} \left[\left[\hat{\mathbf{A}}, \check{I} \right] \right]^K &= \left[\hat{\mathbf{A}}, \hat{I}^K \right] \\ &= \hat{\mathbf{A}} \hat{I}^K - \hat{I}^K \hat{\mathbf{A}}. \end{aligned} \tag{4.44}$$

Substituting $\hat{h} \to \hat{\rho}_m h_m$, multiplying form the left by $\hat{\rho}_n/4$ and taking the trace gives

$$\left[\hat{\mathbf{A}}, \hat{I}^K\right] \to \frac{D_F}{4}\mathrm{Tr}\left\{\hat{I}^K\hat{\rho}_n\hat{\mathbf{A}}\right\} - \frac{D_F}{4}\mathrm{Tr}\left\{\hat{\rho}_n\hat{I}^K\hat{\mathbf{A}}\right\}, \tag{4.45}$$

where we have used that the trace is invariant under a cyclic permutation of the elements in the last term. Writing out the first term in terms of h_m gives

$$\begin{aligned}\frac{D_F}{4}\mathrm{Tr}\left\{\hat{I}^K\hat{\rho}_n\hat{\mathbf{A}}\right\} =& \frac{D_F}{4}\mathrm{Tr}\left\{\hat{g}^R\partial_s\hat{g}^R\hat{\rho}_m\hat{\rho}_n\hat{\mathbf{A}} - \hat{\rho}_m\hat{g}^A\partial_s\hat{g}^A\hat{\rho}_n\hat{\mathbf{A}}\right\}h_m \\ &+ \frac{D_F}{4}\mathrm{Tr}\left\{\hat{\rho}_m\hat{\rho}_n\hat{\mathbf{A}} - \hat{g}^R\hat{\rho}_m\hat{g}^A\hat{\rho}_n\hat{\mathbf{A}}\right\}\partial_s h_m \\ &- \frac{iD_F}{4}\mathrm{Tr}\left\{\hat{g}^R\hat{\mathbf{A}}\hat{g}^R\hat{\rho}_m\hat{\rho}_n\hat{\mathbf{A}} - \hat{\rho}_m\hat{g}^A\hat{\mathbf{A}}\hat{g}^A\hat{\rho}_n\hat{\mathbf{A}}\right\}h_m,\end{aligned} \tag{4.46}$$

while we for the second term have

$$\begin{aligned}\frac{D_F}{4}\mathrm{Tr}\left\{\hat{\rho}_n\hat{I}^K\hat{\mathbf{A}}\right\} =& \frac{D_F}{4}\mathrm{Tr}\left\{\hat{\rho}_n\hat{g}^R\partial_s\hat{g}^R\hat{\rho}_m\hat{\mathbf{A}} - \hat{\rho}_n\hat{\rho}_m\hat{g}^A\partial_s\hat{g}^A\hat{\mathbf{A}}\right\}h_m \\ &+ \frac{D_F}{4}\mathrm{Tr}\left\{\hat{\rho}_n\hat{\rho}_m\hat{\mathbf{A}} - \hat{\rho}_n\hat{g}^R\hat{\rho}_m\hat{g}^A\hat{\mathbf{A}}\right\}\partial_s h_m \\ &- \frac{iD_F}{4}\mathrm{Tr}\left\{\hat{\rho}_n\hat{g}^R\hat{\mathbf{A}}\hat{g}^R\hat{\rho}_m\hat{\mathbf{A}} - \hat{\rho}_n\hat{\rho}_m\hat{g}^A\hat{\mathbf{A}}\hat{g}^A\hat{\mathbf{A}}\right\}h_m.\end{aligned} \tag{4.47}$$

We write this more compactly with

$$\begin{aligned}\left[\hat{\mathbf{A}}, \hat{I}^K\right] =& \left(Q^L_{nm} - Q^R_{nm}\right)h_m + \left(M^L_{nm} - M^R_{nm}\right)\partial_s h_m \\ &- i\left(S^L_{nm} - S^R_{nm}\right)h_m, \end{aligned} \tag{4.48a}$$

$$Q^L_{nm} = \frac{D_F}{4}\mathrm{Tr}\left\{\hat{g}^R\partial_s\hat{g}^R\hat{\rho}_m\hat{\rho}_n\hat{\mathbf{A}} - \hat{\rho}_m\hat{g}^A\partial_s\hat{g}^A\hat{\rho}_n\hat{\mathbf{A}}\right\}, \tag{4.48b}$$

$$Q^R_{nm} = \frac{D_F}{4}\mathrm{Tr}\left\{\hat{\rho}_n\hat{g}^R\partial_s\hat{g}^R\hat{\rho}_m\hat{\mathbf{A}} - \hat{\rho}_n\hat{\rho}_m\hat{g}^A\partial_s\hat{g}^A\hat{\mathbf{A}}\right\}, \tag{4.48c}$$

$$M^L_{nm} = \frac{D_F}{4}\mathrm{Tr}\left\{\hat{\rho}_m\hat{\rho}_n\hat{\mathbf{A}} - \hat{g}^R\hat{\rho}_m\hat{g}^A\hat{\rho}_n\hat{\mathbf{A}}\right\}, \tag{4.48d}$$

$$M^R_{nm} = \frac{D_F}{4}\mathrm{Tr}\left\{\hat{\rho}_n\hat{\rho}_m\hat{\mathbf{A}} - \hat{\rho}_n\hat{g}^R\hat{\rho}_m\hat{g}^A\hat{\mathbf{A}}\right\}, \tag{4.48e}$$

$$S^L_{nm} = \frac{D_F}{4}\mathrm{Tr}\left\{\hat{g}^R\hat{\mathbf{A}}\hat{g}^R\hat{\rho}_m\hat{\rho}_n\hat{\mathbf{A}} - \hat{\rho}_m\hat{g}^A\hat{\mathbf{A}}\hat{g}^A\hat{\rho}_n\hat{\mathbf{A}}\right\}, \tag{4.48f}$$

$$S^R_{nm} = \frac{D_F}{4}\mathrm{Tr}\left\{\hat{\rho}_n\hat{g}^R\hat{\mathbf{A}}\hat{g}^R\hat{\rho}_m\hat{\mathbf{A}} - \hat{\rho}_n\hat{\rho}_m\hat{g}^A\hat{\mathbf{A}}\hat{g}^A\hat{\mathbf{A}}\right\}. \tag{4.48g}$$

We can now construct an expression for the arc length derivative of the modes of the Keldysh component of the matrix current, I_n, with

$$\partial_s I_n = -V_{nm}h_m + i\left\{Q^{LR}_{nm}h_m + M^{LR}_{nm}\partial_s h_m - iS^{LR}_{nm}h_m\right\}, \tag{4.49}$$

where we have introduced the shorthand $X^{LR}_{nm} = X^L_{nm} - X^R_{nm}$. This is to be set equal to the arclength derivative of eq. (4.39a), with

$$\begin{aligned}\partial_s I_n =& M_{nm}\partial_s^2 h_m \\ &+ (Q_{nm} + \partial_s M_{nm} - iS_{nm})\partial_s h_m \\ &+ (\partial_s Q_{nm} - i\partial_s S_{nm})h_m\end{aligned} \tag{4.50}$$

Combining the above equations, we finally arrive at an equation for h_m

$$\begin{aligned} M_{nm}\partial_s^2 h_m = &-(V_{nm} + \partial_s Q_{nm})\, h_m \\ &-(Q_{nm} + \partial_s M_{nm})\, \partial_s h_m \\ &+ i\left(Q^{LR}_{nm} - iS^{LR}_{nm} + \partial_s S_{nm}\right) h_m \\ &+ i\left(M^{LR}_{nm} + S_{nm}\right) \partial_s h_m. \end{aligned} \tag{4.51}$$

We may completely isolate h_m by multiplying both sides by the inverse of M_{nm}.

The advantage of this parametrization is, as observed in ref. [60], not only the explicit form of the equation — see e. g. ref. [65] where the equation is only implicit — but all quantities except for h_m can be determined beforehand.

Furthermore, it is observed in ref. [60] from the expression for the Keldysh component of the matrix current, eq. (4.39a), that Q_{nm} corresponds to contributions from the supercurrent, as the h_m terms can be non-zero in equilibrium. A spatially varying distribution matrix implies resistive current, and hence M_{nm} corresponds to the resistive contribution. The argument extends to the terms that depend on the spin-orbit field.

As a final note, in decomposing $\hat{h}$, ref. [60] notes that the traces $\hat{\rho}_n \hat{1}^K$ *are proportional to spectral charge, spin, heat, and spin-heat currents*. This does not hold in our case, as we selected the matrices spanning spin-space, $\hat{\sigma}_i$, such that they did not depend on position. Only the modes relating to quasiparticle energy and charge, $\hat{\rho}_0 \hat{1}^K$ and $\hat{\rho}_4 \hat{1}^K$ respectively, carry a direct physical interpretation. We may of course extract the relevant traces with, e. g. $\hat{\sigma}_T$, after calculating the distribution matrix to, e. g. compare with the uncurved case.

BOUNDARY CONDITIONS The Kupriyanov -Lukichev boundary conditions of section 4.3 can be applied to this particular parametrization of the equation in a similar manner. These will also depend only on equilibrium quantities [60].

Spesifically, we will be voltage-biasing a normal-metal reservoir, which is done mathematically by having the distribution matrix of the normal metal, $\hat{h}_N$, given as $\mathrm{diag}\,(h_+, h_+, h_-, h_-)$ with $h_\pm = \tanh(\epsilon \pm eV/2T)$. The framework allows for spin-dependent voltages and temperatures, as well as temperature gradients, but this is outside the scope of this thesis.

5 PHYSICAL SYSTEMS

This chapter will bridge the gap between the mostly general considerations of the previous chapter, to sloving the Usadel equation for spesific geometries with spesific parameters.

The physical observables we will be considering are those of the equilibrium supercurrent, and the magnetization of the wire. Introducing curvature into the system, we may alter the spin-structure of the charge flowing through the juncton, and in turn generate long range triplets for long range currents [45]. The magnetization profile of our wire is a manifestation of the anisotripic behaviour of the long range triplet correlations. The magnetizatio profile is also tunable by applying a voltage bias.

5.1 Classes of curves

In this section, we will introduce the arc-length parametrization for some classes of curves for which we solve the Usadel equation in chapter 6. As a simple example, we will consider at a circular arc, while the focus is on curves where the curvature function are different linear combiations of logistic function, which we in this context should think of as a generalization of a the step function. This way we can investigate geometries that are curved in one end, and where the curvature function is symmetric or antisymmetric around the middle of the ferromagnetic regions.

CIRCULAR ARC For a circular arc, the curvature is constant, $\kappa(s) = \kappa$; this can be shown fairly simply by solving the Frenet-Serret equations. This is the system that was studied in ref [45], and we will for easy reference use the same parametrization of the curves.

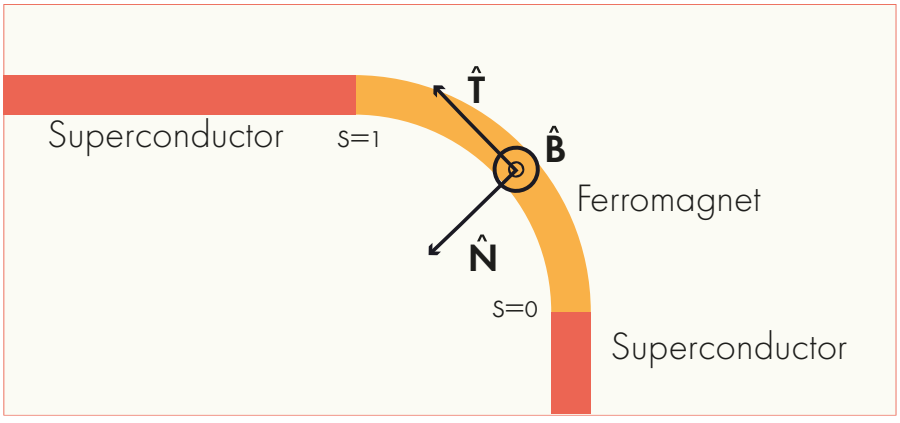

Figure 5.1: Schematic of an SFS system where the ferromagnetic region is curved in a circular arc. The unit vectors are given as a function of the arclength, s. With the circular arc, the curvature is constant with $\kappa(s) = \kappa$

We have our arc run counter clockwise in the xy-plane, and set at $s = 0$, $\left\{\hat{\mathbf{T}}, \hat{\mathbf{N}}, \hat{\mathbf{B}}\right\} = \{\hat{\mathbf{y}}, -\hat{\mathbf{x}}, \hat{\mathbf{z}}\}$. Then, by eq. (3.17) we have a parametrization for the tangentent vector and its (bi)normal given by

$$\hat{\mathbf{T}}(s) = -\sin(\kappa \cdot s)\,\hat{\mathbf{x}} + \cos(\kappa \cdot s)\,\hat{\mathbf{y}} \tag{5.1a}$$

$$\hat{\mathbf{N}}(s) = -\cos(\kappa \cdot s)\,\hat{\mathbf{x}} - \cos(\kappa \cdot s)\,\hat{\mathbf{y}} \tag{5.1b}$$

$$\hat{\mathbf{B}}(s) = \hat{\mathbf{z}} \tag{5.1c}$$

This corresponds to the arc given by

$$\mathbf{r}(s) = \kappa^{-1}(1 - \cos(\kappa \cdot s))\hat{\mathbf{x}} + \kappa^{-1}\sin(\kappa \cdot s)\,\hat{\mathbf{y}} \tag{5.2}$$

where we have chosen $\mathbf{r}(s = 0)$ to be the origin.

Transforming the Pauli-matrices to the Frenet-Serret-frame is done by,

$$\sigma_{T,N,B}(s) = \boldsymbol{\sigma} \cdot \left\{\hat{\mathbf{T}}(s), \hat{\mathbf{N}}(s), \hat{\mathbf{B}}(s)\right\}, \tag{5.3}$$

meaning

$$\sigma_T = -\sin(\kappa \cdot s) \cdot \sigma_x + \cos(\kappa \cdot s)\,\sigma_y = \begin{pmatrix} 0 & -ie^{i\kappa s} \\ ie^{i\kappa s} & 0 \end{pmatrix}, \tag{5.4a}$$

$$\sigma_N = -\cos(\kappa \cdot s)\,\sigma_x - \cos(\kappa \cdot s)\,\sigma_y = \begin{pmatrix} 0 & -e^{i\kappa s} \\ e^{i\kappa s} & 0 \end{pmatrix}, \tag{5.4b}$$

$$\sigma_B = \sigma_z = \begin{pmatrix} 1 & 0 \\ 0 & -1 \end{pmatrix}. \tag{5.4c}$$

Considering the expression we had for the exchange field contribution to the self energy, eq. (3.43), we have

$$\hat{\Sigma}_{FM} = \eta^{ij} h_i \hat{\sigma}_j, \tag{5.5}$$

which is similar to having the exchange field rotate at constant rate in space.

LOGISTIC CURVATURE FUNCTIONS The main focus is on curves with curvature functions we build from logistic curvature functions. We should think of the logistic functions as smoother version of step-functions, which is suitable to describe diffusive systems in the quasiclassical regime, where it is a prerequisite that the self energy terms varies slowly compared to the Fermi wavelength.

The physical interpretation is that we curve some section of the wire. THe conceptually simplest thing to do is to curve only one end; this will be a starting point for considering an anisotropic geometry without symmetry. If we curve both ends, we have the choice of curving the two ends in the same or opposite direction; this corresponds to having a curvature function that is symmetric or anti-symmetric around the midpoint, and allows us to study anisotropic systems with some symmetry.

We name these curves from their shapes, with the wire curved in only one end as *J-like*, and the two others as *S-* and *C-like* curves.

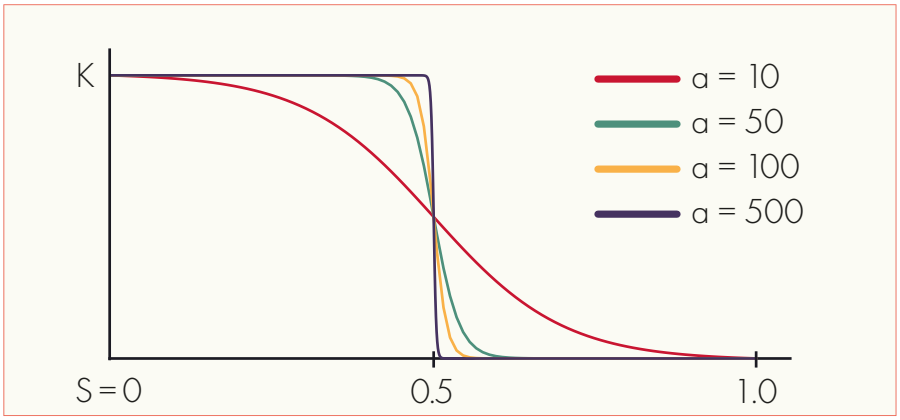

Figure 5.2: Logistic functions with different shape parameters, a. Here, the offset is fixed at $s = 0.5$ and scaled by a factor,K, representing the magnitude of the curvature.

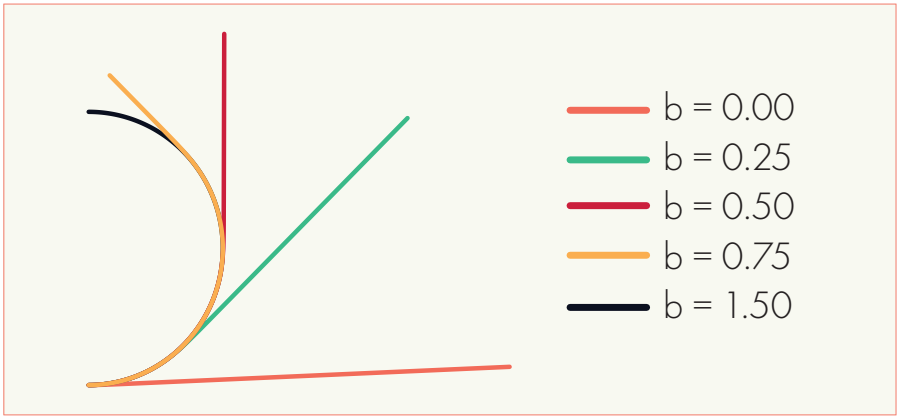

Figure 5.3: Curves generated from eq. (5.6), meaning $\kappa(s) = K(1 - l(s; a, b))$, with $s \in [0, 1]$ – meaning the curve length is fixed as well. Here we have fixed the shape parameter, $a = 50$, and magnitude parameter $K = \pi$, and vary the offset b. The offset controls how long the curve follows the circular arc.

J-LIKE CURVE A starting point is what we will refer to as a *J-like* curve. Here

$$\kappa(s) = K\left(1 - l(s; a, b)\right), \tag{5.6}$$

$$l(s; a, b) = \frac{e^{a(s-b)}}{1 + e^{a(s-b)}}, \tag{5.7}$$

where we refer to K as the *curvature amplitude*, l as a logistic function with *shape parameter* a and *offset* b. The function is plotted for different values of the shape parameter, a, in fig. 5.2.

Picking the same intital values of $\hat{T}, \hat{N}, \hat{B}$ as with the circular arc, the basis vectors are given as

$$\begin{aligned}\hat{\mathbf{T}}(s) = &-\sin\left[\frac{K}{a}\left(as + L(s; a, b)\right)\right]\hat{\mathbf{x}}, \\ &+\cos\left[\frac{K}{a}\left(as + L(s; a, b)\right)\right]\hat{\mathbf{y}}\end{aligned} \tag{5.8a}$$

$$\begin{aligned}\hat{\mathbf{N}}(s) = &-\cos\left[\frac{K}{a}\left(as + L(s; a, b)\right)\right]\hat{\mathbf{x}}, \\ &-\sin\left[\frac{K}{a}\left(as + L(s; a, b)\right)\right]\hat{\mathbf{y}}\end{aligned} \tag{5.8b}$$

$$\hat{\mathbf{B}}(s) = \hat{z}. \tag{5.8c}$$

with

$$L(s; a, b) = \ln\left(\frac{1 + e^{-ab}}{1 + e^{a(s-b)}}\right). \tag{5.9}$$

The relationship between the curvature function, $\kappa(s)$ and the curve, $\mathbf{r}(s)$, is a little opaque. Mathematically,

$$\mathbf{r}(s) = \mathbf{r}(0) + \int_0^s \hat{\mathbf{T}}(\sigma)\mathrm{d}\sigma, \tag{5.10}$$

meaning there are two sets of integration between $\kappa(s)$ and $\mathbf{r}(s)$. The relationship is especially opaque with this particular choice of $\kappa(s)$ — as there exist no analytical function for $\mathbf{r}$. For a fixed shape parameter $a = 50$ and magnitude of curvature $K = \pi$, some curves, $\mathbf{r}(s)$, with different offsets are shown in fig. 5.3.

One way to think of these curves are that they follow the path of some circular arc of radius $1/K$ for an arclength of b, and then follow a straight path. As to not change curvature instantaneously, the shape parameter a determines the length scale over which the "decoupling" from the circular arc happens, with the limit $a \to \infty$ corresponding to leaving the arc instantaneously.

The J-like curve is in some sense a building block for the S- and C- curves which we will consider. It is also in the limit, $b > L$, a circular arc. This allows us continuously traverse the parameter space, e. g. from a straight wire to a circular arc, with the curvature never being spatially uniform.

S- AND C-LIKE CURVES As we are studying SFS-junctions, we may also consider geometries where both ends of the ferromagnetic region is curved.

To do so with our logistic functions, we could consider curvature functions that are symmetric and antisymmetric if we invert them by the junction midpoint; this will be the *S- and C-like* curves respectively.

Here the curvature functions are

$$\kappa(s) = \kappa(s) = K\left(1 - l(s; a, b) \mp l(s; a', b')\right), \quad b' > b, \tag{5.11}$$

$$l(s; a, b) = \frac{e^{a(s-b)}}{1 + e^{a(s-b)}}, \tag{5.12}$$

the $-$ corresponds to a S-like curve, and the curvature function $\kappa(s)$ is antisymmetric when $b' = 1 - b$ and $a = a'$. The $+$ branch corresponds to a C-like curve where the curvature function is symmetric under the same conditions.

The equations for the Frenet-Serret basis vectors are similar to eq. (5.8), but with an extra L term, and similarly for the Pauli matrices.

Translated to real space, these curvature functions correspond to curves with a S- and C- like shape in the sense that there is a straight section with ends that curve in the opposite or same direction. With $b' = 1 - b$ and $a = a'$, the S-like curve has *twofold rotation symmetry*, with rotations around the point $\mathbf{r}(s = 0.5)$, while the C-like curve has a *mirror plane* spanned by $\hat{N}$ and $\hat{B}$ for $s = 0.5$. Apart from some complications regarding the shape parameter, the C-like curves turns to a smooth circular with radius of curvature equal to $R = 1/K$, while the S-like curve gets

With $b > b' \simeq 0.5$, the C-curve turns unhelpful, as the tails of the logistic function will overlap and increase the local curvature beyond K. This does not mean that the curve necessarily intersects itself, but the picture of two curved regions separated by a straight region breaks down.

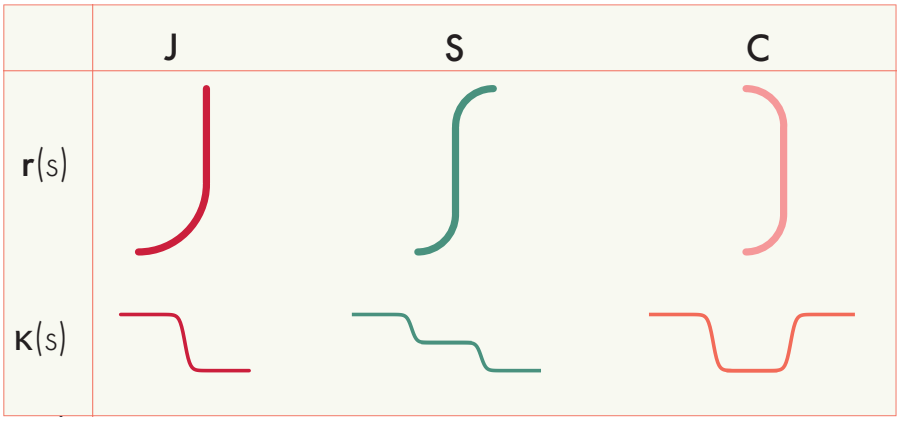

Figure 5.4: Schematic of J-, S- and C like curves, $\mathbf{r}(s)$, with their associated curvature function, $\kappa(s)$.

5.2 Equilibrium Current

As menitoned in section 1.1, a phase difference, $\phi = \varphi_R - \varphi_L$ between the superconductors of a, e. g. SFS, junction [13, 66]. In our constext, we should understand this as succesive *Andreev reflections* leading to a net transport of Cooper pairs from one superconductor to the other. With the reflections being a phase coherent process, so is the transport. In the tunneling limit, i. e. our interfaces are relativly opaque, the current varies sinusoidaly with the phase difference,

$$I(\phi) = I_c \sin(\phi), \tag{5.13}$$

where we refer to I_c as the critical current.

Introducing magnetic order will also introduce spatial modulation of the wave function, which may shift the ground state of the system from $\phi = 0$ to $\phi = \pi$. This in trun shifts the sign of I_c [66], with current running in the opposite direction. Control over the junction ground state may be an important part of spintronic circuit elements [67, 68].

The charge current in our 1D wires without spin orbit coupling, given as [65]

$$I_Q = I_{Q_0} \int_{-\infty}^{\infty} d\epsilon \, \mathrm{Tr}\{\hat{\tau}_3 \, [\check{g}\partial_z \check{g}]\}, \tag{5.14}$$

where $I_{Q_0} = N_0 D_F A|\Delta|e/4L$, with N_0 the density of states at the Fermi level in the absence of an exchange field and superconducting correlations, D_F the diffusion constant, A the area we are considering, $|\Delta|$ the magnitude of the bulk superconducting gap, e the electron charge and L the length of the wire we are considering.

In equilibrium, the expression simplifies to

$$I_Q = I_{Q_0} \int_{-\infty}^{\infty} d\epsilon \, \mathrm{Tr}\left\{\hat{\tau}_3 \left(\hat{g}^R \partial_s \hat{g}^R - \hat{g}^A \partial_s \hat{g}^A\right)\right\} \tanh\left(\frac{\epsilon}{2k_B T}\right), \tag{5.15}$$

where we have used the ansatz from ,

$$\hat{g}^K = \left(\hat{g}^R - \hat{g}^A\right) \tanh\left(\frac{\epsilon}{2k_B T}\right). \tag{5.16}$$

By writing out the retared and advanced Green's functions, $\hat{g}^{R,A}$, it is possible to show that the current depends only on the anomalous Green's function, $\underline{f}$, i. e. the off-diagonal blocks from eq. (2.12), as such

$$I_Q = 2I_{Q_0} \int_{-\infty}^{\infty} d\epsilon \, \mathrm{Tr}\left\{\tilde{f}\partial_s f - f\partial_s \tilde{f}\right\} \tag{5.17}$$

where we have supressed the $\underline{\cdot}$ to not clutter the equation too much. We may in further decompose the anomalous Green's function in terms of a *singlet* and *triplet component* as such [69][1]

$$f = (f_0 + \mathbf{d}\cdot\boldsymbol{\sigma})\, i\sigma_2, \tag{5.18}$$

1 Generally, we have $f = (f_0 + \eta^{ij} d_i \sigma_j)\, i\sigma_2$. The fact that σ_2 appears and is independent of the Frenet-Serret basis vectors is a result of the inner product being independent of the choice of coordinate system.

with $\mathbf{d} = (d_T, d_N, d_B)$ as the *d-vector* and f_0 as the singlet component. With the anomalous Green's function f, decomposed, we may also decompse the the current, I_Q, into singlet and triplet components. This is conventionally done as such [45, 69]

$$\begin{aligned}\frac{I_0}{I_{Q_0}} &= -8\int_0^\infty d\epsilon\, \mathrm{Re}\left\{\tilde{f}_j \partial_s f_0 - f_0 \partial_s \tilde{f}_0\right\} \tanh\left(\frac{\epsilon}{2k_B T}\right), \\ \frac{I_j}{I_{Q_0}} &= 8\int_0^\infty d\epsilon\, \mathrm{Re}\left\{\tilde{d}_j \partial_s d_j - d_j \partial_s \tilde{d}_j\right\} \tanh\left(\frac{\epsilon}{2k_B T}\right),\end{aligned} \tag{5.19a}$$

with I_j corresponding to triplets aligned with the j-direction. Crucially, these current components only sum to the total charge current if $\mathbf{d} \cdot \partial_s \boldsymbol{\sigma} = 0$. This is illustrated by considering

$$\partial_s f = (\partial_s f_0 + (\partial_s \mathbf{d}) \cdot \boldsymbol{\sigma} + \mathbf{d} \cdot \partial_s \boldsymbol{\sigma})\, i\sigma_2. \tag{5.20}$$

Considering only our planar curves with $\tau(s) = 0$

$$\begin{aligned}\mathbf{d} \cdot \partial_s \boldsymbol{\sigma} &= d_T \partial_s \sigma_T + d_N \partial_s \sigma_N + d_B \partial_s \sigma_B, \\ &= d_T \kappa(s) \hat{N} - d_N \kappa(s) \hat{T},\end{aligned} \tag{5.21a}$$

where the derivatives are determined from eq. (3.17). This term will in term give rise to an additional current contribution [45, 69]

$$I_\kappa = 16\kappa(s) \int_0^\infty d\epsilon\, \mathrm{Re}\left\{\tilde{d}_N d_T - \tilde{d}_T d_N\right\} \tanh\left(\frac{\epsilon}{2k_B T}\right), \tag{5.22}$$

which should be understood as a function of the (energy dependent) difference in (complex) argument of the elements of the d-vector [45]. That is, we require the d-vector to rotate in spin-space for I_κ to be non-zero. For clarity, rotation of the d-vector will convert short range triplet correlations, d_T, to long ranged ones d_N. The last component, d_B, is zero with $\partial_s \sigma_B = 0$. For a more physical interpretation, the term decribes an inverse *Edelstein effect* [69].

5.3 Magnetization

In the superconductor-ferromagnet junctions, the proximity effect induces a non-uniform distribution of triplet correlations. This distribution can be tuned by applying a voltage bias [65].

To better understand the effects of applying the bias, and hence the non-equilibrium properties of the system, we may want to decouple the proximity induced equilibrium magnetization from the spin accumulation induced by the voltage bias.

We consider first the total magnetization, M_s. With the Keldysh Green's function $\hat{g}^K = \hat{g}^R\hat{h} - \hat{h}\hat{g}^A$, we can determine the magnetization in direction $\hat{\mathbf{u}}$, as [65, 70]

$$M_u(s) = M_0 \int_\infty^\infty d\epsilon\, \mathrm{Tr}\left\{\hat{\mathbf{u}}\, \mathrm{diag}\left(\underline{\boldsymbol{\sigma}}, \underline{\boldsymbol{\sigma}}^*\right) \hat{g}^K\right\}. \tag{5.23}$$

Here, $M_0 = g\mu_B N_0 |\Delta|/16$, with g being the g-factor of electrons, μ_B the Bohr magneton, N_0 the density of states at the Fermi level in the absence of an

exchange field and $|\Delta|$ the superconducting gap. Similarly to ref. [65], we refer to eq. (5.23) as the *total spin accumulation*.

The non-equilibrium contribution is given as

$$M'_u(s) = M_0 \int_\infty^\infty d\epsilon \, \mathrm{Tr}\left\{\hat{\mathbf{u}} \, \mathrm{diag}\left(\underline{\sigma}, \underline{\sigma}^*\right)\left(\hat{g}^K - \hat{g}^K_{eq}\right)\right\}, \tag{5.24}$$

with $\hat{g}^K_{eq} = \left(\hat{g}^R - gA\right)\tanh\left(\epsilon/2k_B T\right)$.

The magnetization in eq. (5.23) includes the spin accumulation directly induced by the proximitized superconductor as well a contribution that is induced by the applied voltage bias, which we refer to as an *equilibrium* and *nonequilibrium contribution* respectively. The equilibrium contribution

6 NUMERICAL RESULTS

6.1 Equilibrium current

CHOICE OF PARAMETERS We consider a superconductor-ferromagnet-superconductor (SFS) structure. For the simulations, we select the temperature $T = 0.005T_c$. We assume Kuprianov-Lukichev boundary conditions, with the additional assumption of the bulk superconductor solution to the Usadel equation on the superconducting side of the interface. The interface resistance parameter is set to $\zeta_0 = \zeta_L = 3$ for both interfaces. For the parametrization of the S- and C-like curves, we set the offset $b' = 1 - b$, and shape parameter $a = 30$. The Usadel equation is solved in the ferromagnetic region which has length L, such that $s \in (0, L)$. We pick the convention for the superconducting phase difference, ϕ, such that will be such that the superconductor at $s = 0$ has "absolute" phase $\varphi_0 = -\phi/2$ and that at $s = L$ has $\varphi_1 = +\phi/2$.

The available parameter space is then the length of the ferromagnetic region, L, the exchange field $\mathfrak{h}$ and the offset, b, and choice of curve shape.

NUMERICAL RESULTS In ref. [45], a $0 - \pi$ transition was induced by having a by curving a wire of fixed length along circular arcs of smaller and smaller radii. These results are replicated in fig. 6.1 (a). We may trace a different path in the parameter space with the same endpoints by means of the J-shaped curve. This is shown in figure 6.1 (b), where we plot the current components at $s = L/2$ as a function of the offset, b. Keep in mind that the total charge current is constant throughout the ferromagnetic region, the current components vary. This might be especially misleading at low offsets for the J-like curves, as e. g. the long range triplet component, I_N, and the Edelstein component I_κ, decays relatively quickly as the curvature function, $\kappa(s)$ goes to zero.

With the C-like curve, figure 6.1c, we also follow a path in parameter space with similar starting and endpoints as for the J-like curve and circular arc. With $b = 0.5$, the C-like curve is exactly equal to the circular arc with $\kappa = \pi$.[1]

One of the findings of [45], was that the curvature at which the $0 - \pi$ transition took place depended on the length of the junction. Similarly, the transition depends on the symmetry of the junction. Observe that the $0 - \pi$ that it happens at different offsets for the J and C-like curves. This is even if we account for the fact that at equal offsets, twice the length of the C-like curve is non-straight. Thus, geometric configurations where the critical current disappears depend not only on the curvature magnitude, but also the shape of the curvature function.

The symmetries of the S- and C-like curves are in some sense opposite. As discussed in section 3.2 the curvature function, $\kappa(s)$, is symmetric and anti-symmetric during inversion around the point $s = L/2$ for C- and S-like curves respectively. Geometrically this translates to two-fold rotation

1 This does not hold for for $b = 0$, as the tail of the logistic function is within the ferromagnetic region.

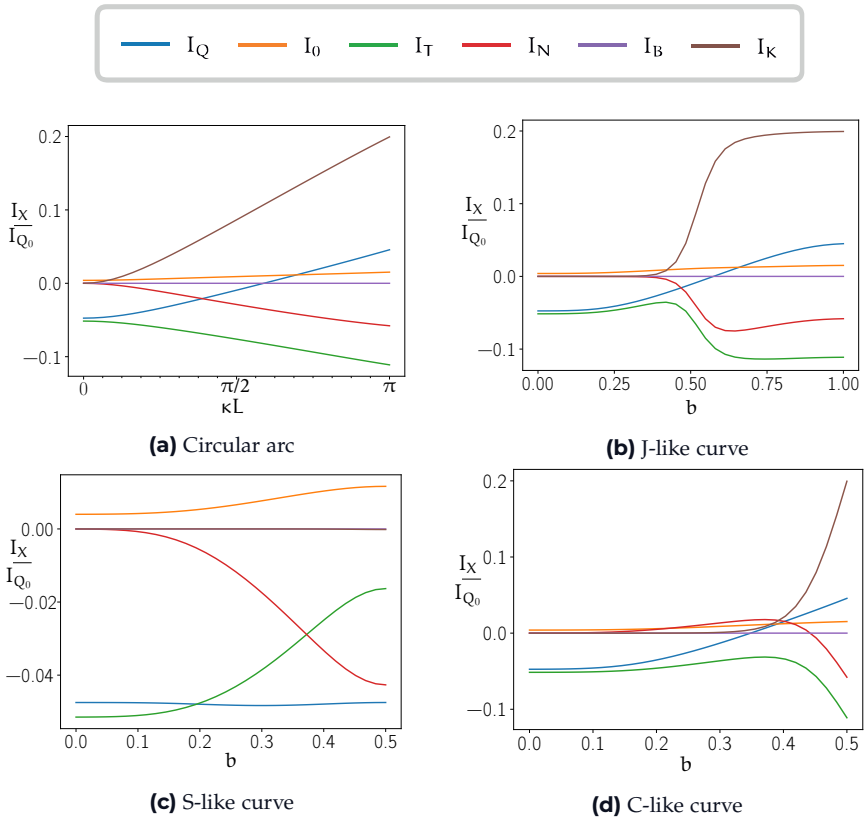

(a) Circular arc

(b) J-like curve

(c) S-like curve

(d) C-like curve

Figure 6.1: Current components, I_X as a function of (a) curvature amplutide, κ, and (b,c,d) offset at $s = L/2$ at critical current. The geometries are (a) a circular arc, (b) J-, (c) S-, and (d) C-, like curves, with $L = 2.0\xi$, $h = |\Delta|\hat{T}$.

symmetry for the for the S-like curve, and a mirror plane for the C-like curve. Physically, in the S-like curve, the d-vector is rotated in one direction on one side, and the opposite direction on the other side. For the C-like curve, it is rotated in the same direction in both curved regions.

The spatial variations of the different current compoents, I_X, for different choice of junction length,L, and curvature amplitude, K, for S- and C- like curves are given in fig. A.1. The most striking difference is that the (spatial) derivatives of singlet, I_0, and short range triplet, I_T, components changes signs multiple times for the C-like curves, but only once for the S-like curves. This corresponds to the derivatives of the curvature function being an even function around $s = L/2$ for the S-like curve, and an odd function for the C-like curve. This picture complcates somewhat with longer curves, as the spin-mixing goes through multiple cycles.

The current-offset relation for the S-like curve, fig. 6.1, is more curious than its J- and C-like counterparts; the charge current changes very little as a function of the offset. As we will get back to, this is in general not true for S-like curves, but corresponds to a choice of parameters in which the effects of spin-mixing and the rotation of the d-vector do not interact, i. e. they do in conjunction not display an effect on the charge current. The rate of rotaion of the d-vector scales with the local curvature function, while the rate of the spin mixing depends on the strength of the exchange field. With these parameters, the introduction of curvature does rotate the d-vector, but at such a speed to not meaningfully affect the triplet-to-singlet spin mixing.

Notably, the introduction of curvature may for the S-like curves enhance the total charge current, I_Q. In fig. 6.2, we are considering an S-like curve, where we have, compared to fig. 6.1, increased both the length and curvature amplitude to, $L = 4.0\xi$ and $K = 2\pi$. Both parameters are doubled, and in the limit $b = 0.5$, this geometry roughly corresponds to two semi-circles curving in the opposite direction. Here the effects of spin mixing and the rotation of the d-vector interact constructively to both enhance the charge current, I_Q, but also the long range triplet component, I_N, in the centre of the junction.

In ref. [45], it was also predicted that the introduction of curvature could increase the equilibrium current by a similar magnitude for the same material parameters, including the length of the junction. However, as discussed earlier, the system of ref. [45] underwent a $0 - \pi$ transition as curvature was introduced, with the π state carrying a larger critical current, whereas ours underwent no such transition. The explanation given in ref. [45] is that as curvature is introduced, the triplet component changes sign while the singlet component does not. This is further illustrated in the phase-current relationship, fig. 6.2 (c) and (d), in which the singlet component disappears with the introuction of curvature.

In the region with the offset $b \sim 0.5$ of figure 6.2 a, the equilibrium current decreases as b is increases. This is the region where the tails of the logistic functions overlap, and should not be intrepreted to mean there is some optimal curvature for the generation of long range triplets. We would expect such an optimum to correspond to parameters where our physical assumptions break down, e. g. where the junction curves enough to intersect itself; although not shown here, the critical current increases with the curvature amplitude in the system of figure 6.2(a).

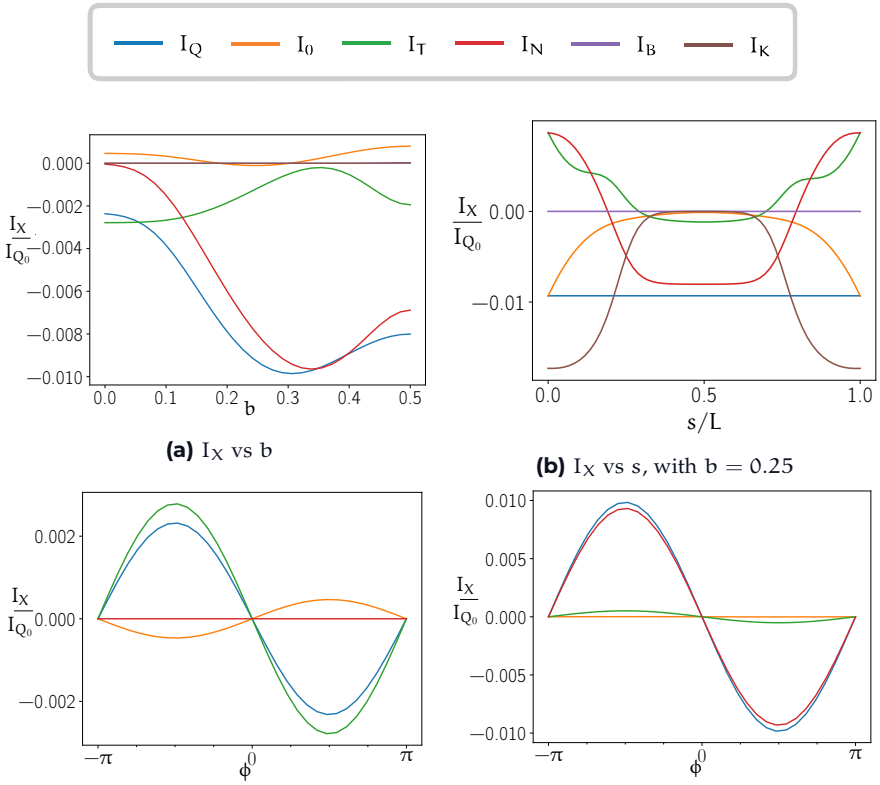

(a) I_X vs b

(b) I_X vs s, with $b = 0.25$

(c) Phase current relationship with $K = 0$

(d) Phase current relationship with $K = 2\pi$

Figure 6.2: (a) Current components, I_X, as a funcfion of offset, S like curve with $L = 4.0\xi, K = 2\pi, \mathbf{h} = |\Delta|\hat{T}$. (b) current components, I_X as a fucntion of position with offset $b = 0.25$, (c, d) current phase relationship at curvature amplutide (c) $K = 0$ and $K = 2\pi$.

6.2 Magnetization

CHOICE OF PARAMETERS To study the the magnetization, we will consider an SFN junction, such that the system in a steady state when voltage biased [71]. We select interface resistance parameters $\zeta_0 = 3$, $\zeta_L = 15$, with the superconductor at the $s = 0$ interface; this ensures that the superconducting proximity effect dominates in the voltage biased system. We also set the temperature $T = 0.005T_c$.

We consider only circular arcs, with $\kappa(s) = \kappa$, and limit ourselves to having the exchange field in the tangential direction, $\mathbf{h} \| \hat{\mathbf{T}}$, and fix the length of the ferromagnetic region to $L = 0.8\xi$. With this choice of the length L, we ensure that superconducting correlations are present throughout the ferromagnetic region, and that the voltage drop largely happens at the interfaces.

NUMERICAL RESULTS Briefly limiting ourselves to equilibrium, the introduction of spin orbit coupling to the system can alter the magnetization of the ferromagnetic region, which is shown in section 6.2 (a). As can be seen in section 6.2(b), the introduction of curvature gives a similar effect. Notably, for circular arcs, the geometric considerations limit us to the region $\kappa \leqslant \pi$.

Applying a voltage bias to the system, the magnetization varies along the curve. The open question is how or if the curvature effects this altered magnetization. section 6.2 shows how the total spin accumulation depends on the applied bias for curvatures of $\kappa L = 0$ and $\kappa L = \pi$.

While both values of κ allows for the inversion of the magnetization with applied bias, the total spin accumulation of the curved structure is more anisotripic and consentrated in one region. Here, it is important to note the curvature of lines in the plot at constant voltage, and to observe that the non-equilibrium magnetization, section 6.2 (c) and (d), exhibits this peaked behaviour in the curved system. This is an indication that the effects of curvature and voltage bias interact.

At low biases, the equilibrium contribution dominates, with the non-equilibrium contribution, M_s', close to zero. The bias at which the non-equilibrium contribution becomes significant does not seem to depend directly on curvature. This is further corroborated in figure A.2, where increasing the curvature does not change the bias where magnetization changes significantly, but increasing the magnitude of the exchange field does. This observation is in line with [65], in which *[...] a smalll increase in the [exchange] field strength may either shift the maximal magnetization towards higher bias values, or enhance magnetization without a bias shift, [...]*, although the systems studied are slightly different.

To summarise, the findings do demonstrate curvature controlled spin accumulation profiles, that can be tuned by a voltage bias and exchange field.

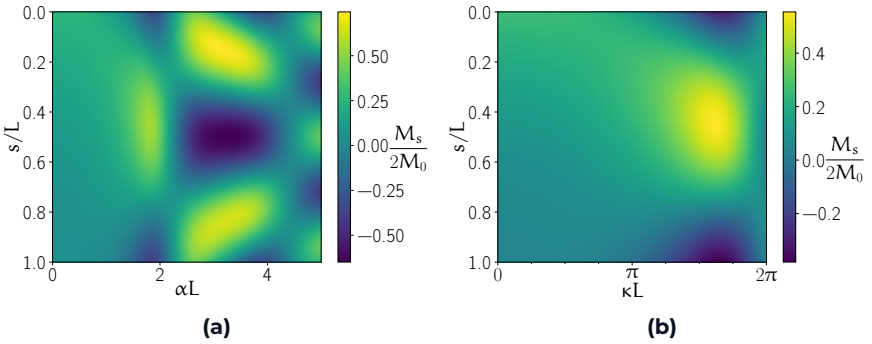

Figure 6.3: Magnetization along the tangential direction of the wire, M_s, in an SFN junction as a function of (a) the spin orbit constant α with curvature function $\kappa = 0$ and (b) the curvature $\kappa(s) = \kappa$ with $L = 0.8\xi T = 0.005Tc$, $\mathbf{h} = \Delta\hat{T}$ and $\hat{\mathbf{A}} = (\alpha(\sigma_B - \sigma_N), 0, 0)$. The magnetization is calculated on a uniform 96×60 grid, with gaussian interpolation between the points.

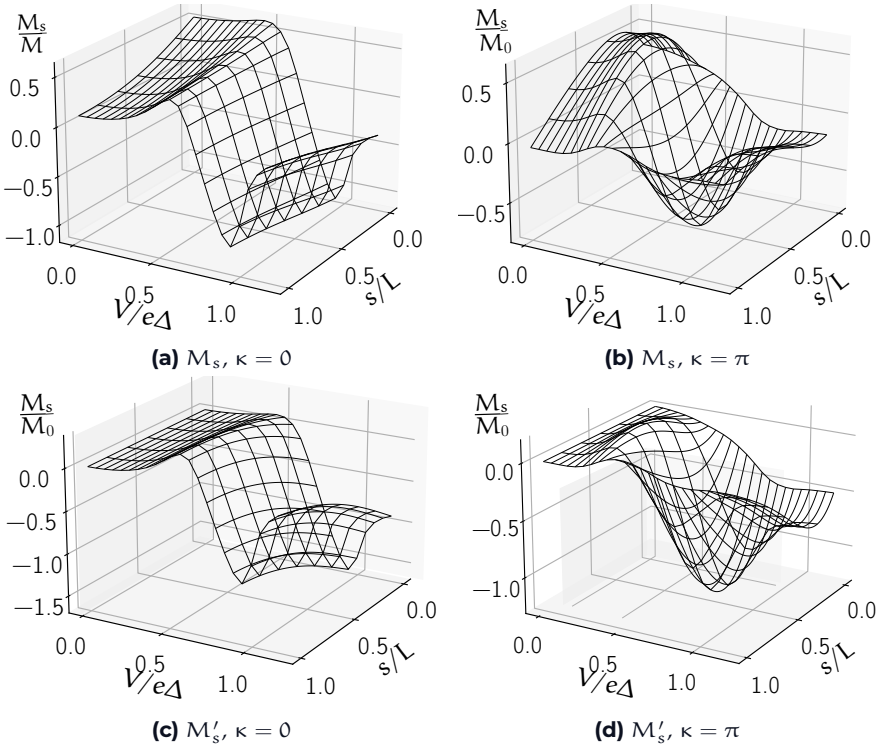

Figure 6.4: Total magnetization, M_s, and non-equilibrium contribution , M_s', along the tangential direction of a wire in an SFN junction with $L = 0.8\xi$, $T = 0.005T_c$, $\zeta_0 = 3$ on the superconducting side, and $\zeta_L = 15$ on the metal side.

7 SUMMARY AND OUTLOOK

The generation of long-range spin triplet correlations from superconductor-ferromagnet heterostructures may be a candidate for spintronic applications, offering the prospect of supercurrents carrying net spin. Introducing curvature to such systems may, through the introduction of a quantum geometric potential and strain induced spin orbit interactions, generate these spin triplet correlations.

In this thesis, we rederived the Usadel equation for planar curves with a non-zero spin orbit field in terms of the arc-length derivate. We also parametrized the quantum kinetic equations to study non-equilibrium properties of the system.

We found the equilibrium current to be tuneable by means of curvature. The equilibrium current could be enhanced, and the junction could undergo a $0-\pi$ transition depending on the (geometric) symmetry of the junction. Furthermore, we found curvature dependent spin-accumulation profiles that could be further tuned by applying a voltage bias to the system or altering the exchange field strength. Increasing the curvature resulted in increasingly peaked distributions of spin accumulation. It should be stressed that the curvature affected both the equilibrium and non-equilibrium properties of the system.

FUTURE WORK In addition to more thoroughly exploring the parameter(s) spaces we have investigated, there are some additonal questions close to the subject matter that have yet to be investigate. Chiefly the effect of curvature on the conductance in the voltage biased system, as well as the spin accumulation in geometries of non-uniform curvature. The numerical framework we have used is directly applicable to explore these question.

Another, although less related question, is the relationship between the critical temperature and curvature. In ref. [46], it was shown that introducing curvature could tune the critical temperature; only 1D wires curved along some circular arc were assesed. A next step may be to assess the critical temperature in structures with anisotropic curvature amplitude, e. g. the S-like curves we have studied. To study the critical temperature requires us to solve the Usadel equation self consistently in both the superconducting and ferromagnetic region.

A less related, but open, question is the effect of curvature on the converision from resistive to supercurrent in voltage biased junctions; this also requires us to solve the Usadel equation (self consistently) on the superconducting side of the interface as well as the ferromagnetic side. It is assumed in ref. [60] that the converision chiefly happens inside the superconductor and in some sense as a function of the superconducting contribution to the self energy.

In this thesis, we limited ourselves to 1D planar curves, which comes with the restriction that they are not to intersect. For the spesific geometries we considered, this placed a limit on the magnitude of curvature. Considering

a spiral wire [72] instead, we could investigate the properties of wires with multiple windings.

Adding torsion or another dimention of transport to the Usadel equation gives additional geometric degrees of freedom. Without torsion, we are limited to planar curves, placing limis on how to make curves such that they do not intersect. The requirement that curves cannot intersect can also be relaxed with additional dimentions of transport, where we may join or proximitize different junctions.

Adding a non-zero torsion function requires us to rederive the Usadel equation and alter the implementation of the slover, whereas we should be employing some *finite difference scheme* [73, 74] for systems with 2- or 3 dimension of transport.

A SUPPLEMENTARY FIGURES

A.1 Equilibrium current

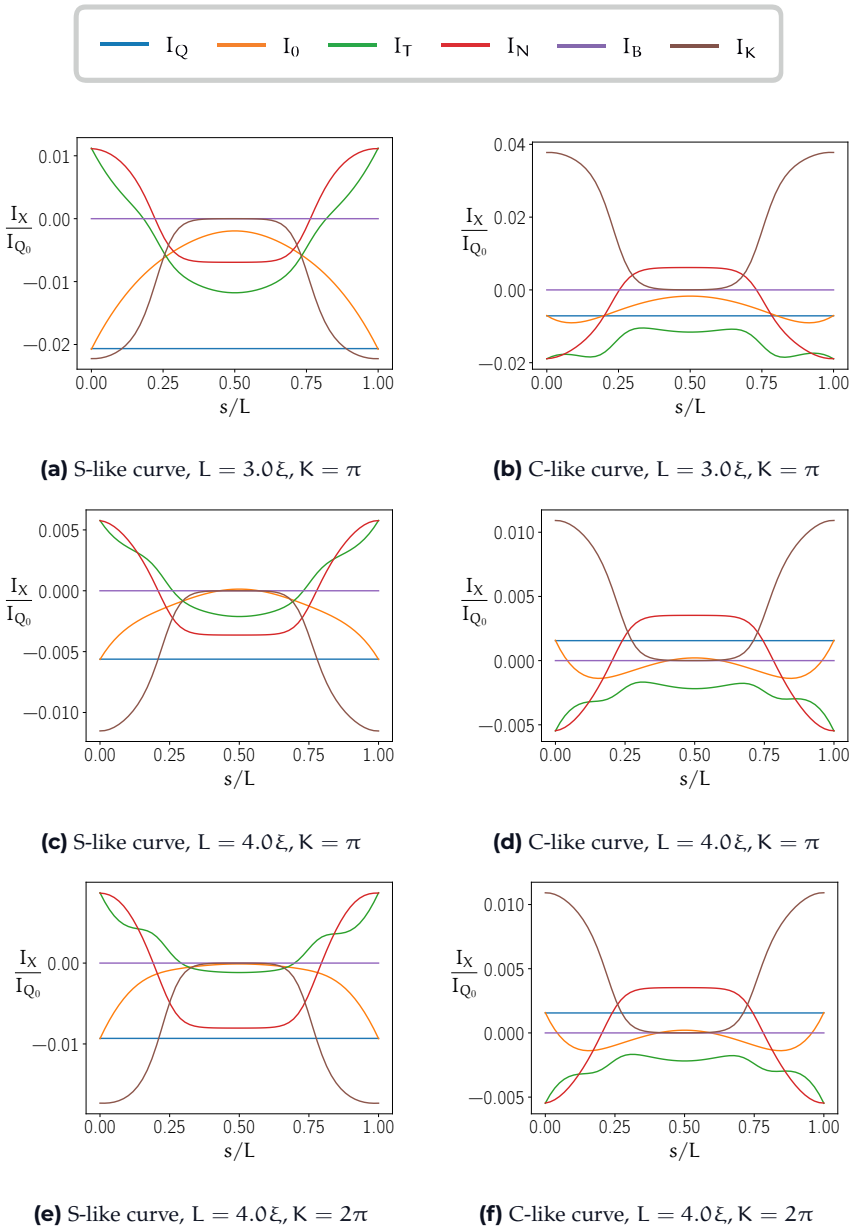

(a) S-like curve, $L = 3.0\xi$, $K = \pi$

(b) C-like curve, $L = 3.0\xi$, $K = \pi$

(c) S-like curve, $L = 4.0\xi$, $K = \pi$

(d) C-like curve, $L = 4.0\xi$, $K = \pi$

(e) S-like curve, $L = 4.0\xi$, $K = 2\pi$

(f) C-like curve, $L = 4.0\xi$, $K = 2\pi$

Figure A.1: Spatial variation of the equilibrium current components, I_X, at critical current, $\phi = \pi/2$ for (a,c,e) S- or (b,d,f) C- like SFS-junctions with $b = 0.25$. The interface resistance parameters are, $\zeta_0 = \zeta_1 = 3$, the temperature $T = 0.005T_c$ and exchange field $h = \Delta\hat{T}$.

A.2 Non-equilibrium magnetization

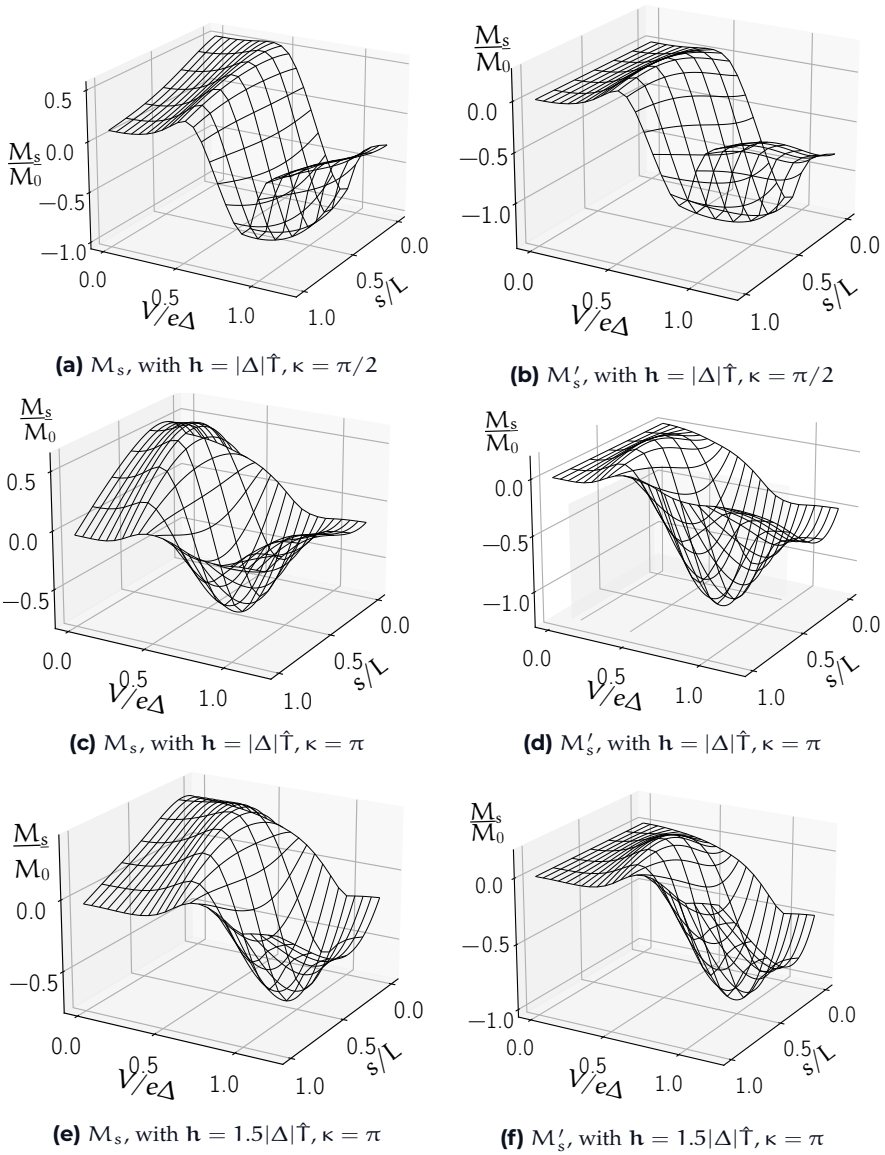

(a) M_s, with $h = |\Delta|\hat{T}, \kappa = \pi/2$

(b) M_s', with $h = |\Delta|\hat{T}, \kappa = \pi/2$

(c) M_s, with $h = |\Delta|\hat{T}, \kappa = \pi$

(d) M_s', with $h = |\Delta|\hat{T}, \kappa = \pi$

(e) M_s, with $h = 1.5|\Delta|\hat{T}, \kappa = \pi$

(f) M_s', with $h = 1.5|\Delta|\hat{T}, \kappa = \pi$

Figure A.2: Total magnetization, M_s, and non equilibrium contribution to the magnetization, M_s' along the tangential direction as a function of position s/L and voltage bias V. The junctions are curved along a circular arc with radius of curvature $1/\kappa$, has temperature $T = 0.005T_c$ and length $L = 0.8\xi$.

BIBLIOGRAPHY

[1] Y. Lvovsky and P. Jarvis. "Superconducting systems for MRI-present solutions and new trends." In: *IEEE Transactions on Applied Superconductivity* 15.2 (2005), pp. 1317–1325. DOI: 10.1109/TASC.2005.849580.

[2] J. Clarke and A. Braginski. *The SQUID handbook*. Vol. 1. Wiley Online Library, 2004. ISBN: 9783527603640.

[3] J. Linder and J.W.A. Robinson. "Superconducting spintronics." In: *Nature Physics* 11.4 (2015), pp. 307–315. DOI: 10.1038/nphys3242.

[4] G. Yang, C. Ciccarelli, and J. W.A. Robinson. "Boosting spintronics with superconductivity." In: *APL Materials* 9.5 (2021), p. 050703. DOI: https://doi.org/10.1063/5.0048904.

[5] H.K. Onnes. "Further experiments with Liquid Helium. G. On the Electrical Resistance of Pure Metals, etc. VI. On the Sudden Change in the Rate at which the Resistance of Mercury Disappears." In: *Through Measurement to Knowledge*. Springer, 1991, pp. 267–272.

[6] J. Bardeen, L. N. Cooper, and J. R. Schrieffer. "Theory of superconductivity." In: *Physical review* 108.5 (1957), p. 1175.

[7] M. Tinkham. *Introduction to superconductivity*. Dover Publications Inc, 2004. ISBN: 978-0486435039.

[8] C. Kittel and P. McEuen. *Introduction to solid state physics*. 8th ed. Wiley New York, 1996. ISBN: 0-471-41526-X.

[9] P. Weiss. "L'hypothèse du champ moléculaire et la propriété ferromagnétique." In: *Journal de Physique Théorique et Appliquée* 6.1 (1907), pp. 661–690. DOI: 10.1051/jphystap:019070060066100.

[10] J.A. Ouassou. "Manipulating superconductivity in magnetic nanostructures in and out of equilibrium." PhD thesis. NTNU, 2019. ISBN: 978-82-326-3738-8.

[11] A.F. Andreev. "Thermal conductivity of the intermediate state of superconductors II." In: *Sov. Phys. JETP* 20 (1965), p. 1490.

[12] M. J. M. de Jong and C. W. J. Beenakker. "Andreev Reflection in Ferromagnet-Superconductor Junctions." In: *Phys. Rev. Lett.* 74 (9 1995), pp. 1657–1660. DOI: 10.1103/PhysRevLett.74.1657.

[13] A. I. Buzdin. "Proximity effects in superconductor-ferromagnet heterostructures." In: *Rev. Mod. Phys.* 77 (3 2005), pp. 935–976. DOI: 10.1103/RevModPhys.77.935.

[14] P. Fulde and R. A. Ferrell. "Superconductivity in a Strong Spin-Exchange Field." In: *Phys. Rev.* 135 (3A 1964), A550–A563. DOI: 10.1103/PhysRev.135.A550.

[15] A.I. Larkin and I.U.N. Ovchinnikov. "Inhomogeneous state of superconductors(Production of superconducting state in ferromagnet with Fermi surfaces, examining Green function)." In: *Soviet Physics-JETP* 20 (1965), pp. 762–769.

[16] M. Houzet and A. I. Buzdin. "Long range triplet Josephson effect through a ferromagnetic trilayer." In: *Phys. Rev. B* 76 (6 2007), p. 060504. DOI: 10.1103/PhysRevB.76.060504.

[17] T.S. Khaire et al. "Observation of Spin-Triplet Superconductivity in Co-Based Josephson Junctions." In: *Phys. Rev. Lett.* 104 (13 2010), p. 137002. DOI: 10.1103/PhysRevLett.104.137002.

[18] J. W. A. Robinson, J. D. S. Witt, and M. G. Blamire. "Controlled Injection of Spin-Triplet Supercurrents into a Strong Ferromagnet." In: *Science* 329.5987 (2010), pp. 59–61. DOI: 10.1126/science.1189246.

[19] J.W.A. Robinson, Z. H. Barber, and M.G. Blamire. "Strong ferromagnetic Josephson devices with optimized magnetism." In: *Applied Physics Letters* 95.19 (2009), p. 192509. DOI: 10.1063/1.3262969.

[20] M. Eschrig. "Spin-polarized supercurrents for spintronics." In: *Physics Today* 64.1 (2011), pp. 43–49. ISSN: 00319228. DOI: 10.1063/1.3541944.

[21] F. S. Bergeret and I. V. Tokatly. "Singlet-Triplet Conversion and the Long-Range Proximity Effect in Superconductor-Ferromagnet Structures with Generic Spin Dependent Fields." In: *Phys. Rev. Lett.* 110 (11 2013), p. 117003. DOI: 10.1103/PhysRevLett.110.117003.

[22] F. S. Bergeret and I. V. Tokatly. "Spin-orbit coupling as a source of long-range triplet proximity effect in superconductor-ferromagnet hybrid structures." In: *Phys. Rev. B* 89 (13 2014), p. 134517. DOI: 10.1103/PhysRevB.89.134517.

[23] M. Duckheim and P. W. Brouwer. "Andreev reflection from noncentrosymmetric superconductors and Majorana bound-state generation in half-metallic ferromagnets." In: *Phys. Rev. B* 83 (5 2011), p. 054513. DOI: 10.1103/PhysRevB.83.054513.

[24] Y. A. Bychkov and E. I. Rashba. "Oscillatory effects and the magnetic susceptibility of carriers in inversion layers." In: *Journal of Physics C: Solid State Physics* 17.33 (1984), pp. 6039–6045. DOI: 10.1088/0022-3719/17/33/015.

[25] G. Dresselhaus. "Spin-Orbit Coupling Effects in Zinc Blende Structures." In: *Phys. Rev.* 100 (2 1955), pp. 580–586. DOI: 10.1103/PhysRev.100.580.

[26] Lev Petrovich Gor'kov. "Microscopic derivation of the Ginzburg-Landau equations in the theory of superconductivity." In: *Sov. Phys. JETP* 9.6 (1959), pp. 1364–1367.

[27] J. Rammer and H. Smith. "Quantum field-theoretical methods in transport theory of metals." In: *Rev. Mod. Phys.* 58 (2 1986), pp. 323–359. DOI: 10.1103/RevModPhys.58.323.

[28] W. Belzig et al. "Quasiclassical Green's function approach to mesoscopic superconductivity." In: *Superlattices and Microstructures* 25.5 (1999), pp. 1251–1288. ISSN: 0749-6036. DOI: https://doi.org/10.1006/spmi.1999.0710.

[29] G. Eilenberger. "Transformation of Gorkov's equation for type II superconductors into transport-like equations." In: *Zeitschrift für Physik A Hadrons and nuclei* 214.2 (1968), pp. 195–213. DOI: 10.1007/bf01379803.

[30] K. D. Usadel. "Generalized diffusion equation for superconducting alloys." In: *Physical Review Letters* 25.8 (1970), p. 507.

[31] V. Chandrasekhar. *Superconductivity: Volume 1: Conventional and Unconventional Superconductors*. Springer Science & Business Media, 2008. Chap. 8, Proximity-Coupled Systems: Quasiclassical Theory of Superconductivity. ISBN: 978-3-540-73252-5.

[32] L. V. Keldysh et al. "Diagram technique for nonequilibrium processes." In: *Sov. Phys. JETP* 20.4 (1965), pp. 1018–1026.

[33] E.M. Lifshitz L.P. Pitaevskii. *Course of theoretical physics. vol. 10: Physical kinetics*. Butterworth-Heinemann, 2012. ISBN: 9780080570495.

[34] M. Amundsen. "Proximity effects in superconducting hybrid structures with spin-dependent interactions." PhD thesis. NTNU, 2020. ISBN: 978-82-326-4834-3.

[35] J.W Serene and D Rainer. "The quasiclassical approach to superfluid 3He." In: *Physics Reports* 101.4 (1983), pp. 221–311. DOI: 10.1016/0370-1573(83)90051-0.

[36] H. Bruus and K. Flensberg. *Many-body quantum theory in condensed matter physics: an introduction*. Oxford University Press, 2004.

[37] Jacob Linder, Takehito Yokoyama, and Asle Sudbø. "Role of interface transparency and spin-dependent scattering in diffusive ferromagnet/superconductor heterostructures." In: *Phys. Rev. B* 77 (17 2008), p. 174514. DOI: 10.1103/PhysRevB.77.174514.

[38] Carmine Ortix. "Quantum mechanics of a spin-orbit coupled electron constrained to a space curve." In: *Physical Review B* 91.24 (2015), p. 245412. DOI: 10.1103/PhysRevB.91.245412.

[39] T. Wang, H. Jiang, and H. Zong. "Geometric influences of a particle confined to a curved surface embedded in three-dimensional Euclidean space." In: *Phys. Rev. A* 96 (2 2017), p. 022116. DOI: 10.1103/PhysRevA.96.022116.

[40] P. Gentile, M. Cuoco, and C. Ortix. "Curvature-induced Rashba spin–orbit interaction in strain-driven nanostructures." In: *Spin*. Vol. 3. 03. World Scientific. 2013, p. 1340002. DOI: 10.1142/s201032471340002x.

[41] Theodore Frankel. *The Geometry of Physics: An Introduction*. 2nd ed. Cambridge University Press, 2003. ISBN: 978-1-107-60260-1. DOI: 10.1017/CBO9780511817977.

[42] M. Kachelriess. *Quantum Fields: From the Hubble to the Planck Scale*. Oxford University Press, 2018. ISBN: 978-0-19-880287-7.

[43] W. Kühnel. *Differential geometry*. Vol. 77. American Mathematical Soc., 2015. ISBN: 978-1-4704-2320-9.

[44] J.W. Moffat. "A new nonsymmetric gravitational theory." In: *Physics Letters B* 355.3 (1995), pp. 447–452. ISSN: 0370-2693. DOI: https://doi.org/10.1016/0370-2693(95)00670-G.

[45] T. Salamone et al. "Curvature-induced long-range supercurrents in diffusive superconductor-ferromagnet-superconductor Josephson junctions with a dynamic 0–π transition." In: *Phys. Rev. B* 104 (6 2021), p. L060505. DOI: 10.1103/PhysRevB.104.L060505.

[46] T. Salamone et al. “Curvature control of the superconducting proximity effect in diffusive ferromagnetic nanowires.” In: *Phys. Rev. B* 105 (13 2022), p. 134511. DOI: 10.1103/PhysRevB.105.134511.

[47] W. . Callister Jr and David G. Rethwisch. *Callister's materials science and engineering*. Ninth. John Wiley & Sons, 2015. ISBN: 978-1118319222.

[48] L. D. Landau et al. *Theory of elasticity: volume 7*. Vol. 7. Elsevier, 1986. ISBN: 9780750626330.

[49] C. Ortix et al. “Curvature-induced geometric potential in strain-driven nanostructures.” In: *Phys. Rev. B* 84 (4 2011), p. 045438. DOI: 10.1103/PhysRevB.84.045438.

[50] R. Córdoba et al. “Vertical growth of superconducting crystalline hollow nanowires by He+ focused ion beam induced deposition.” In: *Nano Letters* 18.2 (2018), pp. 1379–1386. DOI: 10.1021/acs.nanolett.7b05103.

[51] M.S. Dresselhaus et al. “Carbon nanotubes.” In: *The physics of fullerene-based and fullerene-related materials*. Springer, 2000, pp. 331–379. DOI: 10.1007/978-94-011-4038-6_9.

[52] J. Bardeen and W. Shockley. “Deformation Potentials and Mobilities in Non-Polar Crystals.” In: *Phys. Rev.* 80 (1 1950), pp. 72–80. DOI: 10.1103/PhysRev.80.72.

[53] I. V. Tokatly. “Equilibrium Spin Currents Non-Abelian Gauge Invariance and Color Diamagnetism in Condensed Matter.” In: *Physical Review Letters* 101.10 (2008), p. 106601. DOI: 10.1103/PhysRevLett.101.106601.

[54] J. Fröhlich and U.M. Studer. “Gauge invariance and current algebra in nonrelativistic many-body theory.” In: *Rev. Mod. Phys.* 65 (3 1993), pp. 733–802. DOI: 10.1103/RevModPhys.65.733.

[55] F. S. Bergeret, A. F. Volkov, and K. B. Efetov. “Odd triplet superconductivity and related phenomena in superconductor- ferromagnet structures.” In: *Reviews of Modern Physics* 77.4 (2005), pp. 1321–1373. DOI: 10.1103/RevModPhys.77.1321.

[56] D.D. Sheka, V.P. Kravchuk, and Y. Gaididei. “Curvature effects in statics and dynamics of low dimensional magnets.” In: *Journal of Physics A: Mathematical and Theoretical* 48.12 (2015), p. 125202. DOI: 10.1088/1751-8113/48/12/125202.

[57] S.H. Jacobsen, J.A. Ouassou, and J. Linder. “Critical temperature and tunneling spectroscopy of superconductor-ferromagnet hybrids with intrinsic Rashba-Dresselhaus spin-orbit coupling.” In: *Physical Review B - Condensed Matter and Materials Physics* 92.2 (2015), pp. 1–24. DOI: 10.1103/PhysRevB.92.024510.

[58] Y. Tanaka and A. A. Golubov. “Theory of the Proximity Effect in Junctions with Unconventional Superconductors.” In: *Phys. Rev. Lett.* 98 (3 2007), p. 037003. DOI: 10.1103/PhysRevLett.98.037003.

[59] A. Bezryadin. “Quantum suppression of superconductivity in nanowires.” In: *Journal of Physics: Condensed Matter* 20.4 (2008), p. 043202. DOI: 10.1088/0953-8984/20/04/043202.

[60] J.A Ouassou, T.D. Vethaak, and Jacob Linder. "Voltage-induced thin-film superconductivity in high magnetic fields." In: *Phys. Rev. Lett.* 110 (11 2013), p. 117003. DOI: 10.1103/PhysRevB.98.144509.

[61] M. Y. Kuprianov and V. Lukichev. "Influence of boundary transparency on the critical current of dirty SS'S structures." In: *Zh. Eksp. Teor. Fiz* 94 (1988), p. 149.

[62] Y. V. Nazarov. "Novel circuit theory of Andreev reflection." In: *Superlattices and Microstructures* 25.5-6 (May 1999), pp. 1221–1231. DOI: 10.1006/spmi.1999.0738.

[63] W. Belzig et al. "Quasiclassical Green's function approach to mesoscopic superconductivity." In: *Superlattices and Microstructures* 25.5-6 (1999), pp. 1251–1288. DOI: 10.1006/spmi.1999.0710.

[64] A. Schmid and G. Schön. "Linearized kinetic equations and relaxation processes of a superconductor near T c." In: *Journal of Low Temperature Physics* 20.1 (1975), pp. 207–227. DOI: 10.1007/BF00115264.

[65] S.H. Jacobsen and J. Linder. "Quantum kinetic equations and anomalous nonequilibrium Cooper-pair spin accumulation in Rashba wires with Zeeman splitting." In: *Phys. Rev. B* 96 (13 2017), p. 134513. DOI: 10.1103/PhysRevB.96.134513.

[66] A. A. Golubov, M. Yu. Kupriyanov, and E. Il'ichev. "The current-phase relation in Josephson junctions." In: *Rev. Mod. Phys.* 76 (2 2004), pp. 411–469. DOI: 10.1103/RevModPhys.76.411.

[67] AK Feofanov et al. "Implementation of superconductor/ferromagnet/-superconductor π-shifters in superconducting digital and quantum circuits." In: *Nature Physics* 6.8 (2010), pp. 593–597. DOI: 10.1038/nphys1700.

[68] E.C. Gingrich et al. "Controllable 0–π Josephson junctions containing a ferromagnetic spin valve." In: *Nature Physics* 12.6 (2016), pp. 564–567. DOI: 10.1038/nphys3681.

[69] M. Amundsen and J. Linder. "Supercurrent vortex pinball via a triplet Cooper pair inverse Edelstein effect." In: *Phys. Rev. B* 96 (6 2017), p. 064508. DOI: 10.1103/PhysRevB.96.064508.

[70] T. Löfwander et al. "Interplay of Magnetic and Superconducting Proximity Effects in Ferromagnet-Superconductor-Ferromagnet Trilayers." In: *Phys. Rev. Lett.* 95 (18 2005), p. 187003. DOI: 10.1103/PhysRevLett.95.187003.

[71] V. Braude and Y. M. Blanter. "Triplet Josephson Effect with Magnetic Feedback in a Superconductor-Ferromagnet Heterostructure." In: *Phys. Rev. Lett.* 100 (20 2008), p. 207001. DOI: 10.1103/PhysRevLett.100.207001.

[72] L. D. Machado, N.M. Bizao R.A.and Pugno, and Douglas S Galvão. "Controlling movement at nanoscale: curvature driven mechanotaxis." In: *Small* 17.35 (2021), p. 2100909. DOI: 10.1002/smll.202100909.

[73] M. Amundsen and J. Linder. "General solution of 2D and 3D superconducting quasiclassical systems: coalescing vortices and nanoisland geometries." In: *Scientific Reports* 6.1 (2016), pp. 1–13. DOI: 10.1038/srep22765.

[74] J.N. Reddy. *Introduction to the finite element method*. McGraw-Hill Education, 2019. ISBN: 978-1-25-986191-8.

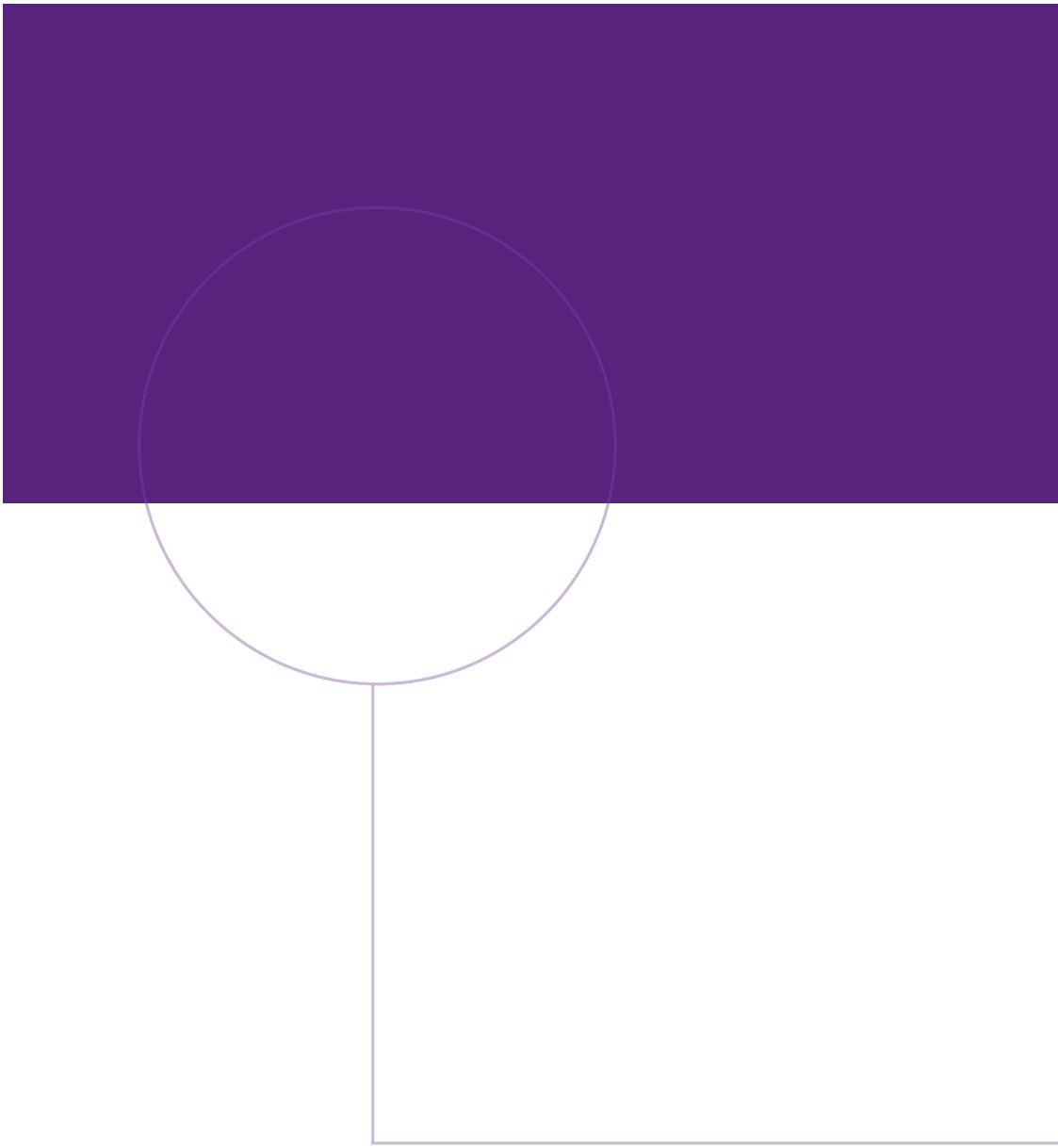

NTNU

Norwegian University of
Science and Technology